

# A GENERAL ALTERNATING-DIRECTION IMPLICIT FRAMEWORK WITH GAUSSIAN PROCESS REGRESSION PARAMETER PREDICTION FOR LARGE SPARSE LINEAR SYSTEMS \*

KAI JIANG<sup>†</sup>, XUEHONG SU<sup>†</sup>, AND JUAN ZHANG<sup>†</sup>

**Abstract.** This paper proposes an efficient general alternating-direction implicit (GADI) framework for solving large sparse linear systems. The convergence property of the GADI framework is discussed. Most of existing ADI methods can be unified in the developed framework. Meanwhile the GADI framework can derive new ADI methods. Moreover, as the algorithm efficiency is sensitive to the splitting parameters, we offer a data-driven approach, the Gaussian process regression (GPR) method based on the Bayesian inference, to predict the GADI framework's relatively optimal parameters. The GPR method only requires a small training data set to learn the regression prediction mapping, can predict accurate splitting parameters, and has high generalization capability. It allows us to efficiently solve linear systems with a one-shot computation, and does not require any repeated computations. Finally, we use the three-dimensional convection-diffusion equation, two-dimensional parabolic equation, and continuous Sylvester matrix equation to examine the performance of our proposed methods. Numerical results demonstrate that the proposed framework is faster tens to thousands of times than the existing ADI methods, such as (inexact) Hermitian and skew-Hermitian splitting type methods in which the consumption of obtaining relatively optimal splitting parameters is ignored. As a result, our proposed methods can solve much larger linear systems which these existing ADI methods have not reached.

**Key words.** general alternating-direction implicit framework, large sparse linear systems, convergent analysis, Gaussian process regression, data-driven method

**AMS subject classifications.** 15A24, 65F10

**1. Introduction.** Large sparse linear systems have wide applications in scientific and engineering computation. To the best of our knowledge, the direct methods, such as Gaussian elimination, QR decomposition, and LU and Cholesky factorizations, have been deeply researched since the 1970s; refer to [6] and the references therein. In practical problems, as the coefficient matrix is often received by discrete or integral operators, it is large scale and sparse. The memory requirements and the difficulties in developing valid parallel implementations can limit the scope especially for large problems. Iterative methods are popular since they have low memory requirements and are easier to parallelize. In this work, our interest is introducing a general alternating-direction implicit (GADI) method to solve large sparse linear systems of the form

$$(1.1) \quad Ax = b,$$

where  $x, b \in \mathbb{C}^n$ ,  $A \in \mathbb{C}^{n \times n}$  is a nonsingular matrix.

**1.1. Background.** Alternating-direction implicit (ADI) methods are widely applied to scientific computation, such as linear systems, partial differential equations

---

\*Submitted to the editors DATE.

**Funding:** The work was supported in part by the National Natural Science Foundation of China (12171412, 11771370), Natural Science Foundation for Distinguished Young Scholars of Hunan Province (2021JJ10037), Hunan Youth Science and Technology Innovation Talents Project (2021RC3110), the Key Project of Education Department of Hunan Province (19A500, 21A0116).

<sup>†</sup> Key Laboratory of Intelligent Computing and Information Processing of Ministry of Education, Hunan Key Laboratory for Computation and Simulation in Science and Engineering, School of Mathematics and Computational Science, Xiangtan University, Xiangtan, Hunan, China, 411105. (Corresponding authors. [kaijiang@xtu.edu.cn](mailto:kaijiang@xtu.edu.cn) (KJ); [zhangjuan@xtu.edu.cn](mailto:zhangjuan@xtu.edu.cn) (JZ)).

(PDEs), and optimization. In the 1950s, Peaceman and Rachford proposed an ADI approach, the Peaceman-Rachford splitting (PRS) method, for solving second-order elliptic equations [18]. Subsequently, Douglas and Rachford developed an efficient method, now named the Douglas-Rachford splitting (DRS) method, for solving heat conduction problems [11]. Since, numerous ADI methods have been presented and applied to solving different PDEs [14, 17]. Besides the application of solving PDEs, ADI methods have also been used in optimization. For instance, a useful optimization method, the alternating-direction method of multipliers, equivalent to the DRS [12], has been widely applied in many fields, such as image science, machine learning, and low-rank matrix completion [16, 22].

The idea of the ADI method has also been devoted to numerical linear algebra [23]. Recently, Bai, Golub, and Ng have offered a Hermitian and skew-Hermitian splitting (HSS) method, analogous to the classical ADI methods in solving PDEs, such as PRS and DRS methods, for non-Hermitian positive definite linear systems [4]. Concretely, they split the coefficient matrix into the Hermitian and non-Hermitian parts through a splitting parameter, and proved that the HSS method is convergent unconditionally to the exact solution of (1.1).

Many researchers have paid much attention to the HSS-type methods in recent years due to its elegant mathematical property, including the normal and skew-Hermitian splitting (NSS) method, the positivedefinite and skew-Hermitian splitting (PSS) method, and the generalized HSS method [5, 7, 8, 9]. Nowadays, these HSS-type methods have been applied to many problems, such as the saddle point system, the matrix equation, the spatial fractional diffusion equation, and the complex semidefinite linear system [3, 10, 25]. A systematical introduction of the HSS-type methods can be found in a recent monograph [6].

**1.2. Challenges.** The ADI methods have attracted extensive interest. However, there still exist several challenges in scheme construction and algorithm efficiency. Existing ADI methods mainly are concern with the concrete matrix splitting formulation. However, there is a lack of a general framework to unify these existing ADI methods, even further offering new ADI schemes. It is the first challenge of the development of ADI methods.

The second challenge is how to choose optimal splitting parameters of ADI methods. ADI methods require splitting the matrix into different parts with splitting parameters. The efficiency of ADI methods is very sensitive to these splitting parameters [2, 4]; also see Figure 3. There are two main methods for selecting parameters. One is traversing parameters or experimental determination within some intervals to obtain relatively optimal parameters [3, 15, 26]. The advantage of this traversal method is that it can obtain relatively accurate optimal parameters, but obviously, it consumes a lot of extra time. Meanwhile, the traversing method is impractical in scientific computation. In practical calculation, it needs to obtain the solution of a one-shot efficient computation, rather than chasing the best algorithmic performance through repeated computations. Another one is estimating relatively optimal parameters through theoretical analysis [4, 24]. Such a theoretical analysis can directly offer a formulation or an algorithm for evaluating splitting parameters. However, the theoretical method is available on a case-by-case basis, and theoretical estimate error heavily affects the algorithmic efficiency. Meanwhile, the theoretical methods may be hardly applicable as the scale of linear system increases.

The third challenge is how to apply ADI methods to efficiently solve large linear systems. The performance of ADI methods is sensitive to splitting matrices and

parameters. For example, the existing results demonstrate that, when ignoring the consumption of obtaining the optimal splitting parameters, the HSS-type methods can solve sparse linear algebraic system of a million levels at best in about a hundred seconds [1], and a continuous Sylvester matrix equation at most 256 order in tens to thousands of seconds [3, 15, 24]. It also should be pointed out that the cost of obtaining these optimal splitting parameters in these ADI methods may be much more expensive than solving the linear system itself. Therefore, it is urgent to improve further the efficiency of ADI schemes to address large linear systems.

**1.3. Contribution.** In this work, we are mainly concerned with the development of ADI methods in solving large sparse linear systems. Our contributions are summarized as follows:

- We put forward a GADI framework to address sparse linear systems, which is more flexible for choosing the splitting matrices and splitting parameters. The new proposed framework can put most existing ADI algorithms into a unified framework and offer new ADI approaches. As an attempt, in this work we present three new ADI methods to solve linear algebraic equations and linear matrix equations. The corresponding convergence properties of the GADI framework and proposed ADI methods are also presented.
- We present a data-driven method to predict relatively optimal splitting parameters, the Gaussian process regression (GPR) method based on Bayesian inference. Concretely, the GPR method learns a mapping from the dimension of linear systems to relatively optimal splitting parameters through a training data set produced from small-scale systems. The GPR method avoids the expensive consumption of traversing parameters, and provides an efficient approach to predicting relatively optimal parameters in practical computation. It should be emphasized that the GPR method requires a small training data set to learning the regression prediction mapping, and has sufficient accuracy and high generalization capability.
- We improve the performance of solving large linear systems by combining the GADI framework and the GPR method. In this work, we take a three-dimensional (3D) convection-diffusion equation, a two-dimensional (2D) parabolic equation (see Appendix A.4), and a continuous Sylvester matrix equation as examples to demonstrate the performance of our proposed methods. In the comparison, we ignore the consumption of obtaining relatively optimal splitting parameters in the classical ADI methods; however, our presented methods can still accelerate the computation within a one-shot computation from tens to thousands of times over these methods. Furthermore, we can apply our methods to solve much larger sparse linear systems which the classical ADI methods have not arrived.

**1.4. Organization and Notations.** The rest of the paper is organized as follows. In section 2, we present the GADI framework to solve linear systems and analyze the convergence properties. Furthermore, we present three new ADI schemes: the GADI-HS, the practical GADI-HS, and the GADI-AB approaches for linear algebra and matrix equations. In section 3, we offer two methods to select the parameters of ADI methods. The first one is the data-driven GPR method based on Bayesian inference. The second one is the theoretical estimation method. In section 4, we illustrate the efficiency of the GADI framework and GPR parameter prediction method through sufficient numerical experiments. Finally, in section 5, we draw some concluding remarks and prospects.

Throughout the paper, the sets of  $n \times n$  complex and real matrices are denoted by  $\mathbb{C}^{n \times n}$  and  $\mathbb{R}^{n \times n}$ , respectively. If  $X \in \mathbb{C}^{n \times n}$ , let  $X^T$ ,  $X^{-1}$ ,  $X^*$ ,  $\|X\|$ ,  $\|X\|_2$ ,  $\|X\|_F$  denote the transpose, inverse, conjugate transpose, determinant, Euclidean norm, and Frobenius norm of  $X$ , respectively. The notations  $\lambda(X) = (\lambda_1(X), \dots, \lambda_n(X))$ ,  $\sigma(X) = (\sigma_1(X), \dots, \sigma_n(X))$ ,  $\rho(X)$  denote the eigenvalue set, singular value set and spectral radius of  $X$ , respectively. The expression  $X > 0$  ( $X \geq 0$ ) means that  $X$  is Hermitian (semi-) positive definite. If  $X, Y \in \mathbb{C}^{n \times n}$ ,  $X > Y$  ( $X \geq Y$ ) denotes that  $X - Y$  is Hermitian (semi-) positive definite.  $\|\cdot\|$  represents the  $L_2$ -norm of a vector. For all  $x \in \mathbb{C}^n$ , denote  $\|x\|_M = \|Mx\|$ . The induced matrix norm is  $\|X\|_M = \|MXM^{-1}\|$ . The symbol  $\otimes$  denotes the Kronecker product.  $I$  represents the identity matrix.

**2. Algorithm framework.** In this section, we first propose the GADI framework to solve linear systems and corresponding convergence analysis. Then we show that these existing ADI schemes belong to the GADI framework. Finally, we give three new ADI schemes: the GADI-HS, the practical GADI-HS algorithms for linear algebraic equations, and the GADI-AB method for matrix equations.

**2.1. GADI framework for linear systems.** In this section, we propose a GADI framework for solving the linear equation (1.1). Let  $M, N \in \mathbb{C}^{n \times n}$  be splitting matrices such that  $A = M + N$ . Given an initial guess  $x^{(0)}$  and  $\alpha > 0$ ,  $\omega \geq 0$ , the GADI framework is

$$(2.1) \quad \begin{cases} (\alpha I + M)x^{(k+\frac{1}{2})} = (\alpha I - N)x^{(k)} + b, \\ (\alpha I + N)x^{(k+1)} = (N - (1 - \omega)\alpha I)x^{(k)} + (2 - \omega)\alpha x^{(k+\frac{1}{2})} \end{cases}$$

for  $k = 0, 1, \dots$

Compared with existing ADI schemes, the GADI framework has more degrees of freedom to construct more ADI methods, including the splitting formulation of matrices  $(M, N)$  and an extra splitting parameter  $\omega$ . To demonstrate the generality of GADI, Table 1 shows the connection between concrete ADI schemes and GADI framework. From Table 1, one can find that the GADI framework contains these

Table 1: Some concrete ADI schemes derived from the GADI framework.

$\omega$	Splitting matrices	ADI method
0	Hermitian and skew-Hermitian	HSS [4]
	Positivedefinite and skew-Hermitian	PSS [5]
	Normal and skew-Hermitian	NSS [5]
	Triangular and skew-Hermitian	TSS [24]
[0, 2)	Hermitian and skew-Hermitian	GADI-HS (2.7)
1	Hermitian and skew-Hermitian	DRS (2.11)
[0, 2)	—	GADI-AB (2.23)

existing ADI schemes. More significantly, the GADI framework can derive new ADI methods by choosing the splitting matrices and splitting parameters, such as the DRS, GADI-HS, and GADI-AB methods as shown in this work.

Next, we analyze the convergence property of the GADI framework.

**LEMMA 2.1.** [4] *Let  $A \in \mathbb{C}^{n \times n}$  be a positive definite matrix, let  $M = \frac{1}{2}(A + A^*)$  and  $N = \frac{1}{2}(A - A^*)$  be its Hermitian and skew-Hermitian parts. Then, the matrix*

$$(2.2) \quad T(\alpha) = (\alpha I + N)^{-1}(\alpha I - M)(\alpha I + M)^{-1}(\alpha I - N)$$

satisfies  $\rho(T(\alpha)) < 1$  for any  $\alpha > 0$ .

LEMMA 2.2. *Let  $M$  be a positive definite matrix, and let  $N$  be a positive (semi-) definite matrix. Then, the matrix defined by (2.2) satisfies  $\rho(T(\alpha)) < 1$  for any  $\alpha > 0$ .*

*Proof.* Let  $\lambda$  and  $\mu$  be the eigenvalues of the matrices  $M$  and  $N$ , respectively. Then the eigenvalues of the matrix  $T(\alpha)$  have the following form

$$v = \frac{\alpha - \lambda}{\alpha + \lambda} \cdot \frac{\alpha - \mu}{\alpha + \mu}.$$

Note that

$$\left| \frac{\alpha - \mu}{\alpha + \mu} \right| \leq 1$$

for  $N$  is a positive (semi-) definite matrix and  $\alpha > 0$ , it then follows that

$$\rho(T(\alpha)) = \max_{\substack{\lambda \in \sigma(M) \\ \mu \in \sigma(N)}} \left| \frac{\alpha - \lambda}{\alpha + \lambda} \right| \cdot \left| \frac{\alpha - \mu}{\alpha + \mu} \right| \leq \max_{\lambda \in \sigma(M)} \left| \frac{\alpha - \lambda}{\alpha + \lambda} \right|,$$

where  $\sigma(M)$  and  $\sigma(N)$  denote the spectrum of matrices  $M$  and  $N$ , respectively. Analogously, since  $M$  is a positive definite matrix, it is easy to verify that  $\rho(T(\alpha)) < 1$ .  $\square$

Now we discuss the convergence of the GADI framework (2.1).

THEOREM 2.3. *Let  $A \in \mathbb{C}^{n \times n}$  be a positive definite matrix, let  $M = \frac{1}{2}(A + A^*)$  and  $N = \frac{1}{2}(A - A^*)$  be its Hermitian and skew-Hermitian parts; or let  $M$  be a positive definite matrix, and let  $N$  be a positive (semi-) definite matrix. The GADI framework (2.1) is convergent to the unique solution  $x^*$  of the linear equation (1.1) for any  $\alpha > 0$  and  $\omega \in [0, 2)$ . Moreover, the spectral radius  $\rho(T'(\alpha, \omega))$  satisfies*

$$(2.3) \quad \rho(T'(\alpha, \omega)) \leq \frac{1}{2}(\rho(T(\alpha)) + 1) < 1,$$

where

$$(2.4) \quad T'(\alpha, \omega) = (\alpha I + N)^{-1}(\alpha I + M)^{-1}(\alpha^2 I + MN - (1 - \omega)\alpha A),$$

and  $T(\alpha)$  is defined by (2.2).

*Proof.* For  $k = 0, 1, 2, \dots$ , by eliminating  $x^{(k+\frac{1}{2})}$  from the second equation of (2.1), we can rewrite the GADI framework as

$$x^{(k+1)} = T'(\alpha, \omega)x^{(k)} + G(\alpha, \omega),$$

where the iterative matrix  $T'(\alpha, \omega)$  is defined by (2.4) and

$$G(\alpha, \omega) = (2 - \omega)\alpha(\alpha I + N)^{-1}(\alpha I + M)^{-1}b.$$

From (2.4), we obtain

$$\begin{aligned} 2T'(\alpha, \omega) &= 2(\alpha I + N)^{-1}(\alpha I + M)^{-1}(\alpha^2 I + MN - (1 - \omega)\alpha(M + N)) \\ &= (2 - \omega)(\alpha I + N)^{-1}(\alpha I + M)^{-1}(\alpha I - M)(\alpha I - N) \\ &\quad + \omega(\alpha I + N)^{-1}(\alpha I + M)^{-1}(\alpha I + M)(\alpha I + N) \\ &= (2 - \omega)T(\alpha) + \omega I, \end{aligned}$$

where  $(\alpha I + M)^{-1}(\alpha I - M) = (\alpha I - M)(\alpha I + M)^{-1}$ . Therefore,

$$T'(\alpha, \omega) = \frac{1}{2}[(2 - \omega)T(\alpha) + \omega I].$$

Hence, we have the following relationship:

$$\mu_k = \frac{1}{2}[(2 - \omega)\lambda_k + \omega], \quad \mu_k \in \lambda(T'(\alpha, \omega)), \quad \lambda_k \in \lambda(T(\alpha)),$$

where  $\lambda(T'(\alpha, \omega))$  and  $\lambda(T(\alpha))$  denote the eigenvalue set of the matrix  $T'(\alpha, \omega)$  and  $T(\alpha)$ , respectively. Since  $\lambda_k, \mu_k \in \mathbb{C}$ , let  $\lambda_k = a + bi$ , where  $i = \sqrt{-1}$ , then

$$\begin{aligned} |\mu_k| &= \frac{1}{2}\sqrt{(2 - \omega)^2 a^2 + \omega^2 + 2(2 - \omega)a\omega + (2 - \omega)^2 b^2} \\ (2.5) \quad &\leq \frac{1}{2}\sqrt{(2 - \omega)^2(a^2 + b^2) + \omega^2 + 2(2 - \omega)\omega\sqrt{a^2 + b^2}} \\ &= \frac{1}{2}[(2 - \omega)|\lambda_k| + \omega]. \end{aligned}$$

Thus, combining (2.5) with  $\omega \in [0, 2)$ , Lemma 2.1, and Lemma 2.2, we obtain

$$\rho(T'(\alpha, \omega)) \leq \frac{1}{2}[(2 - \omega)\rho(T(\alpha)) + \omega] < 1.$$

This implies that the GADI framework is convergent to the unique solution  $x^*$  of (2.1).  $\square$

In the subsequent subsection, we will present three new ADI schemes: the GADI-HS, practical GADI-HS, and GADI-AB methods derived from the GADI framework.

**2.2. GADI-HS scheme for linear algebraic equations.** Assume that the matrix  $A \in \mathbb{C}^{n \times n}$  in (1.1) is a large sparse non-Hermitian and positive definite matrix. The first proposed ADI scheme in the GADI framework is splitting  $A$  into Hermitian (H) and skew-Hermitian (S) parts. A natural selection is

$$(2.6) \quad H = \frac{A + A^*}{2}, \quad S = \frac{A - A^*}{2}.$$

The GADI framework (2.1) becomes the GADI-HS scheme

$$(2.7) \quad \begin{cases} (\alpha I + H)x^{(k+\frac{1}{2})} = (\alpha I - S)x^{(k)} + b, \\ (\alpha I + S)x^{(k+1)} = (S - (1 - \omega)\alpha I)x^{(k)} + (2 - \omega)\alpha x^{(k+\frac{1}{2})}. \end{cases}$$

In the implementation of the GADI-HS method, the two linear systems of (2.7) are both solved by the direct method. From the properties of H and S, one can find that the GADI-HS method satisfies the conditions of Theorem 2.3. Therefore, the GADI-HS scheme is convergent to the unique solution  $x^*$  of the linear (1.1), as Theorem 2.4 shows.

**THEOREM 2.4.** *The GADI-HS method defined by (2.7) is convergent to the unique solution  $x^*$  of the linear equation (1.1) for any  $\alpha > 0$  and  $\omega \in [0, 2)$ . Moreover, the spectral radius  $\rho(T(\alpha, \omega))$  satisfies*

$$\rho(T(\alpha, \omega)) < 1,$$

where

$$(2.8) \quad T(\alpha, \omega) = (\alpha I + S)^{-1}(\alpha I + H)^{-1}(\alpha^2 I + HS - (1 - \omega)\alpha A).$$

The GADI-HS method is a generalized Hermitian and skew-Hermitian (H-S) splitting scheme. We can obtain different H-S splitting methods through varying  $\omega$ .

**PRS (HSS) scheme** When  $\omega = 0$  in GADI-HS method (2.7), we have the PRS method immediately [18], equivalent to the HSS method [4]. Given an initial guess  $x^0$  and  $\alpha > 0$ , for  $k = 0, 1, 2, \dots$ , until  $x^{(k)}$  is convergent,

$$(2.9) \quad \begin{cases} (\alpha I + H)x^{(k+\frac{1}{2})} = (\alpha I - S)x^{(k)} + b, \\ (\alpha I + S)x^{(k+1)} = (\alpha I - H)x^{(k+\frac{1}{2})} + b. \end{cases}$$

The iterative matrix of PRS (HSS) is

$$(2.10) \quad M(\alpha) = (\alpha I + S)^{-1}(\alpha I - H)(\alpha I + H)^{-1}(\alpha I - S).$$

**DRS scheme** When  $\omega = 1$  in GADI-HS method (2.7), we have the DRS iterative method [11]. Given an initial guess  $x^{(0)}$  and  $\alpha > 0$ , for  $k = 0, 1, \dots$ , until  $x^{(k)}$  is convergent,

$$(2.11) \quad \begin{cases} (\alpha I + H)x^{(k+\frac{1}{2})} = (\alpha I - S)x^{(k)} + b, \\ (\alpha I + S)x^{(k+1)} = Sx^{(k)} + \alpha x^{(k+\frac{1}{2})}. \end{cases}$$

The iterative matrix of DRS is

$$M'(\alpha) = (\alpha I + S)^{-1}(\alpha I + H)^{-1}(\alpha^2 I + HS).$$

**Theorem 2.4** has offered a preliminary conclusion of convergence. Next we analyze the convergent speed of the GADI-HS scheme through exploring a deep relationship on spectral radii between  $T(\alpha, \omega)$  in (2.2) and  $M(\alpha)$  in (2.10).

**THEOREM 2.5.** *Let  $A \in \mathbb{C}^{n \times n}$  be a sparse non-Hermitian and positive definite matrix, and let  $H$  and  $S$  defined by (2.6) be its Hermitian and skew-Hermitian parts. Assume that  $\alpha > 0$ ,  $\omega \in [0, 2)$ ,  $\lambda_k, \mu_k$  are the eigenvalues of  $M(\alpha)$  (see (2.10)) and  $T(\alpha, \omega)$  (see (2.8)). Let  $\lambda_k = a + bi$ , where  $i = \sqrt{-1}$ .*

(i) *If  $|\lambda_k|^2 \leq a$ , then*

$$\rho(M(\alpha)) \leq \rho(T(\alpha, \omega)) < 1.$$

(ii) *If  $a < |\lambda_k|^2$  and  $0 < \omega < \frac{4a^2 - 4a + 4b^2}{(1-a)^2 + b^2}$ , then*

$$\rho(T(\alpha, \omega)) < \rho(M(\alpha)) < 1.$$

*Proof.* By using (2.5), we have

$$\begin{aligned} 4|\mu_k|^2 - 4|\lambda_k|^2 &= (2 - \omega)^2 a^2 + \omega^2 + 2(2 - \omega)a\omega + (2 - \omega)^2 b^2 - 4(a^2 + b^2) \\ &= \omega^2 + 4\omega a - 2\omega^2 a + a^2 \omega^2 + b^2 \omega^2 - 4a^2 \omega - 4b^2 \omega \\ &= [(1 - a)^2 + b^2] \omega^2 - (4a^2 - 4a + 4b^2) \omega. \end{aligned}$$

(i) As  $\omega$  is a nonnegative constant, when  $|\lambda_k|^2 \leq a$ , i.e.,  $4a^2 - 4a + 4b^2 \leq 0$ , then

$$|\lambda_k| \leq |\mu_k|.$$

We obtain

$$\rho(M(\alpha)) \leq \rho(T(\alpha, \omega)) < 1.$$

(ii) When  $a < |\lambda_k|^2$  i.e.,  $4a^2 - 4a + 4b^2 > 0$  and we have  $a^2 + b^2 < 1$ , then

$$0 < \omega < \frac{4a^2 - 4a + 4b^2}{(1-a)^2 + b^2} < 2.$$

Thus

$$[(1-a)^2 + b^2]\omega^2 - (4a^2 - 4a + 4b^2)\omega < 0,$$

which is equivalent to  $[(1-a)^2 + b^2]\omega < (4a^2 - 4a + 4b^2)$ , i.e.,  $|\mu_k| < |\lambda_k|$ . Subsequently, we have

$$\rho(T(\alpha, \omega)) < \rho(M(\alpha)) < 1.$$

The proof is completed.  $\square$

*Remark 2.6.* **Theorem 2.5** proves that the GADI-HS scheme converges faster than or equally to the HSS method. In case (i), the GADI-HS method is simplified to the HSS method by taking  $\omega = 0$ . In case (ii), the spectral radius of the GADI-HS scheme is smaller than the HSS method, which means the GADI-HS method has a faster convergent speed.

### 2.3. Practical GADI-HS scheme for linear algebraic equations.

**2.3.1. Practical GADI-HS scheme.** The GADI-HS method (2.7) requires solving two linear systems with coefficient matrices  $(\alpha I + H)$  and  $(\alpha I + S)$ . Directly solving these linear equations would result in heavy computational cost, especially for large-scale systems. An approach to overcome this problem is developing efficient iterative methods to calculate the subproblems.

Concretely, we employ iterative methods to approximately solve  $\tilde{x}^{(k+\frac{1}{2})}$  by

$$(2.12) \quad (\alpha I + H)\tilde{x}^{(k+\frac{1}{2})} \approx (\alpha I - S)\tilde{x}^{(k)} + b$$

and approximately solve  $\tilde{x}^{(k+1)}$  through

$$(2.13) \quad (\alpha I + S)(\tilde{x}^{(k+1)} - \tilde{x}^{(k)}) \approx \alpha(2 - \omega)(\tilde{x}^{(k+\frac{1}{2})} - \tilde{x}^{(k)}).$$

**Algorithm 2.1** summarizes the above practical GADI-HS method. Here, we use the conjugate gradient (CG) and the CG method on normal coefficient equation (CGNE) as the inner iterative methods in **Algorithm 2.1**. When  $\omega = 0$ , the practical GADI-HS method becomes the IHSS (inexact HSS) method [3, 4].

---

#### **Algorithm 2.1** Practical GADI-HS method

---

**Require:**  $\alpha, \omega, \varepsilon, H, S, \tilde{r}^{(0)}, \tilde{\varepsilon}_k, \tilde{\eta}_k, K_{max}, k = 0, \tilde{x}^{(0)} = 0$ .

- 1: **while**  $\|\tilde{r}^{(k)}\|_2^2 > \|\tilde{r}^{(0)}\|_2^2 \varepsilon$  or  $k < K_{max}$  **do**
  - 2:  $\tilde{r}^{(k)} = b - A\tilde{x}^{(k)}$ ;
  - 3: Solve  $(\alpha I + H)\tilde{z}^{(k)} \approx \tilde{r}^{(k)}$  such that  $\tilde{p}^{(k)} = \tilde{r}^{(k)} - (\alpha I + H)\tilde{z}^{(k)}$  satisfies  $\|\tilde{p}^{(k)}\| \leq \tilde{\varepsilon}_k \|\tilde{r}^{(k)}\|$ ;
  - 4: Solve  $(\alpha I + S)\tilde{y}^{(k)} \approx \alpha(2 - \omega)\tilde{z}^{(k)}$  such that  $\tilde{q}^{(k)} = \alpha(2 - \omega)\tilde{z}^{(k)} - (\alpha I + S)\tilde{y}^{(k)}$  satisfies  $\|\tilde{q}^{(k)}\| \leq \tilde{\eta}_k \|\alpha(2 - \omega)\tilde{z}^{(k)}\|$ ;
  - 5: Compute  $\tilde{x}^{(k+1)} = \tilde{x}^{(k)} + \tilde{y}^{(k)}$ ;
  - 6:  $k = k + 1$ .
  - 7: **end while**
-



**2.3.2. Convergence of Practical GADI-HS.** In this section, we discuss the convergent properties of the practical GADI-HS method. It is shown that (2.12) and (2.13) are equivalent to the symmetric form of two-step splitting iteration, which can lead to the subsequent conclusion.

LEMMA 2.7. For linear system (1.1), assume that  $A = M_1 - N_1 = M_2 - N_2$ . Let  $\{\tilde{x}^{(k)}\}$  be an iterative sequence defined by

$$(2.14) \quad \begin{aligned} \tilde{x}^{(k+\frac{1}{2})} &= \tilde{x}^{(k)} + \tilde{z}^{(k)}, & M_1 \tilde{z}^{(k)} &= \tilde{r}^{(k)} + \tilde{p}^{(k)}, \\ \tilde{x}^{(k+1)} &= \tilde{z}^{(k+\frac{1}{2})} + \tilde{x}^{(k+\frac{1}{2})}, & M_2 \tilde{z}^{(k+\frac{1}{2})} &= \tilde{r}^{(k+\frac{1}{2})} + \tilde{q}^{(k+\frac{1}{2})}, \end{aligned}$$

such that

$$\|\tilde{p}^{(k)}\| \leq \tilde{\varepsilon}_k \|\tilde{r}^{(k)}\|, \quad \|\tilde{q}^{(k+\frac{1}{2})}\| \leq \tilde{\eta}_k \|\tilde{r}^{(k+\frac{1}{2})}\|,$$

where  $\tilde{\varepsilon}_k > 0$ ,  $\tilde{\eta}_k > 0$ , and  $\tilde{r}^{(k)} = b - A\tilde{x}^{(k)}$ ,  $\tilde{r}^{(k+\frac{1}{2})} = b - A\tilde{x}^{(k+\frac{1}{2})}$ . Then

$$(2.15) \quad \tilde{x}^{(k+1)} = M_2^{-1}N_2M_1^{-1}N_1\tilde{x}^k + M_2^{-1}(N_2M_1^{-1}+I)b + M_2^{-1}(N_2M_1^{-1}\tilde{p}^{(k)} + \tilde{q}^{(k+\frac{1}{2})}).$$

*Proof.* The proof is in Appendix A.1.  $\square$

Based on Lemma 2.7, we can prove the convergence of the practical GADI-HS.

THEOREM 2.8. Let  $A \in \mathbb{C}^{n \times n}$  be a positive definite matrix,  $H$  and  $S$  in (2.6) be its Hermitian and skew-Hermitian parts,  $\alpha$  be a positive constant, and  $\omega \in [0, 2)$ . Assume that  $\{\tilde{x}^{(k)}\}$  is the iterative sequence generated by Lemma 2.7, and  $\tilde{x}^*$  is the exact solution of (1.1). Then

$$\|\tilde{x}^{(k+1)} - \tilde{x}^*\|_{M_2} \leq (\rho(T(\alpha, \omega)) + \theta_1 \tilde{\varepsilon}_k (\gamma + \theta_2 + \theta_1 \gamma \eta_k) + \theta_1 \gamma \eta_k) \cdot \|\tilde{x}^{(k)} - \tilde{x}^*\|_{M_2}, \quad k = 0, 1, 2,$$

where  $M_1, N_1, M_2, N_2$  are defined in Lemma 2.7, and

$$T(\alpha, \omega) = N_2M_1^{-1}N_1M_2^{-1}, \quad \theta_1 = \|AM_1^{-1}\|, \quad \theta_2 = \|AM_2^{-1}\|, \quad \gamma = \|M_2M_1^{-1}\|.$$

Moreover, if

$$(2.16) \quad \rho(T(\alpha, \omega)) + \theta_2 \varepsilon_{max} (\gamma + \theta_1 + \theta_2 \gamma \eta_{max}) + \theta_2 \gamma \eta_{max} < 1,$$

then  $\{\tilde{x}^{(k)}\}$  is convergent to  $\tilde{x}^*$ , where

$$\eta_{max} = \max_k \{\tilde{\eta}_k\}, \quad \varepsilon_{max} = \max_k \{\tilde{\varepsilon}_k\}.$$

*Proof.* Since  $x^*$  is the exact solution of (1.1), then

$$(2.17) \quad \begin{aligned} \tilde{x}^* &= M_1^{-1}N_1\tilde{x}^* + M_1^{-1}b, \\ \tilde{x}^* &= M_2^{-1}N_2\tilde{x}^* + M_2^{-1}b = M_2^{-1}N_2M_1^{-1}N_1\tilde{x}^* + M_2^{-1}(N_2M_1^{-1} + I)b. \end{aligned}$$

From (2.15), we have

$$(2.18) \quad \begin{aligned} \tilde{x}^{(k+\frac{1}{2})} &= M_1^{-1}N_1\tilde{x}^{(k)} + M_1^{-1}b + M_1^{-1}\tilde{p}^{(k)}, \\ \tilde{x}^{(k+1)} &= M_2^{-1}N_2M_1^{-1}N_1\tilde{x}^k + M_2^{-1}(N_2M_1^{-1} + I)b + M_2^{-1}(N_2M_1^{-1}\tilde{p}^{(k)} + \tilde{q}^{(k+\frac{1}{2})}). \end{aligned}$$

Subtracting the two equations of (2.17) from those of (2.18) reads

$$\begin{aligned}
(2.19) \quad & \|\tilde{x}^{(k+\frac{1}{2})} - \tilde{x}^*\|_{M_2} = \|M_1^{-1}N_1(\tilde{x}^{(k)} - \tilde{x}^*) + M_1^{-1}\tilde{p}^{(k)}\|_{M_2} \\
& \leq \|M_2M_1^{-1}N_1M_2^{-1}\|\|\tilde{x}^{(k)} - \tilde{x}^*\|_{M_2} + \|M_2M_1^{-1}\|\|\tilde{p}^{(k)}\|, \\
& \|\tilde{x}^{(k+1)} - \tilde{x}^*\|_{M_2} = \|M_2^{-1}N_2M_1^{-1}N_1(\tilde{x}^{(k)} - \tilde{x}^*) + M_2^{-1}(N_2M_1^{-1}\tilde{p}^{(k)} + \tilde{q}^{(k+\frac{1}{2})})\|_{M_2} \\
& \leq \|N_2M_1^{-1}N_1M_2\|\|\tilde{x}^{(k)} - \tilde{x}^*\|_{M_2} + \|N_2M_1^{-1}\|\|\tilde{p}^{(k)}\| + \|\tilde{q}^{(k+\frac{1}{2})}\|.
\end{aligned}$$

Note that

$$\|\tilde{r}^{(k)}\| = \|b - A\tilde{x}^{(k)}\| = \|A(\tilde{x}^* - \tilde{x}^{(k)})\| \leq \|AM_2^{-1}\|\|\tilde{x}^{(k)} - \tilde{x}^*\|_{M_2}$$

and

$$\begin{aligned}
\|\tilde{r}^{(k+\frac{1}{2})}\| &= \|b - A\tilde{x}^{(k+\frac{1}{2})}\| = \|A(\tilde{x}^* - \tilde{x}^{(k+\frac{1}{2})})\| \leq \|AM_2^{-1}\|\|\tilde{x}^{(k+\frac{1}{2})} - \tilde{x}^*\|_{M_2} \\
&\leq \|AM_2^{-1}\|(\|M_2M_1^{-1}N_1M_2^{-1}\|\|\tilde{x}^{(k)} - \tilde{x}^*\|_{M_2} + \|M_2M_1^{-1}\|\|\tilde{p}^{(k)}\|).
\end{aligned}$$

By the definitions of  $\{\tilde{p}^{(k)}\}$  and  $\{\tilde{q}^{(k+\frac{1}{2})}\}$  in Lemma 2.7, we have

$$(2.20) \quad \|\tilde{p}^{(k)}\| \leq \tilde{\varepsilon}_k \|r^{(k)}\| \leq \tilde{\varepsilon}_k \|AM_2^{-1}\|\|\tilde{x}^{(k)} - \tilde{x}^*\|_{M_2}$$

and

$$\begin{aligned}
(2.21) \quad & \|\tilde{q}^{(k+\frac{1}{2})}\| \leq \tilde{\eta}_k \|\tilde{r}^{(k+\frac{1}{2})}\| \leq \tilde{\eta}_k \|AM_2^{-1}\|(\|M_2M_1^{-1}N_1M_2^{-1}\| \\
& \quad + \tilde{\varepsilon}_k \|M_2M_1^{-1}\|\|AM_2^{-1}\|)\|\tilde{x}^{(k)} - \tilde{x}^*\|_{M_2}.
\end{aligned}$$

Substituting (2.20) and (2.21) into the second inequality of (2.19) yields

$$\begin{aligned}
& \|\tilde{x}^{(k+1)} - \tilde{x}^*\|_{M_2} \leq \|N_2M_1^{-1}N_1M_2^{-1}\|\|\tilde{x}^{(k)} - \tilde{x}^*\|_{M_2} + \|N_2M_1^{-1}\|\|\tilde{p}^{(k)}\| + \|\tilde{q}^{(k+\frac{1}{2})}\| \\
& \leq \|N_2M_1^{-1}N_1M_2^{-1}\|\|\tilde{x}^{(k)} - \tilde{x}^*\|_{M_2} + \tilde{\varepsilon}_k \|N_2M_1^{-1}\|\|AM_2^{-1}\|\|\tilde{x}^{(k)} - \tilde{x}^*\|_{M_2} \\
& \quad + \tilde{\eta}_k \|AM_2^{-1}\|(\|M_2M_1^{-1}N_1M_2^{-1}\| + \tilde{\varepsilon}_k \|M_2M_1^{-1}\|\|AM_2^{-1}\|)\|\tilde{x}^{(k)} - \tilde{x}^*\|_{M_2} \\
& \leq (\|T(\alpha, \omega)\| + \theta_2\tilde{\varepsilon}_k\|N_2M_1^{-1}\| + \theta_2\tilde{\eta}_k\gamma\|N_1M_2^{-1}\| + \theta_2^2\gamma\tilde{\varepsilon}_k\tilde{\eta}_k)\|\tilde{x}^{(k)} - \tilde{x}^*\|_{M_2} \\
& \leq (\|T(\alpha, \omega)\| + \theta_2\tilde{\varepsilon}_k\|(M_2 - A)M_1^{-1}\| + \theta_2\tilde{\eta}_k\gamma + \theta_2^2\gamma\tilde{\varepsilon}_k\tilde{\eta}_k)\|\tilde{x}^{(k)} - \tilde{x}^*\|_{M_2} \\
& \leq (\|T(\alpha, \omega)\| + \theta_2\tilde{\varepsilon}_k(\|M_2M_1^{-1}\| + \|(AM_1^{-1})\|) + \theta_2\tilde{\eta}_k\gamma + \theta_2^2\gamma\tilde{\varepsilon}_k\tilde{\eta}_k)\|\tilde{x}^{(k)} - \tilde{x}^*\|_{M_2} \\
& \leq (\rho(T(\alpha, \omega)) + \theta_2\tilde{\varepsilon}_k(\gamma + \theta_1 + \theta_2\gamma\tilde{\eta}_k) + \theta_2\gamma\tilde{\eta}_k)\|\tilde{x}^{(k)} - \tilde{x}^*\|_{M_2}.
\end{aligned}$$

From the splitting formulation in Lemma 2.7, it is easy to verify that  $\|N_1M_2^{-1}\| \leq 1$ . Therefore, the fourth inequality in the above expression is hold. Obviously, if the condition (2.16) is met, then  $\{\tilde{x}^{(k)}\}$  is convergent to  $\tilde{x}^*$ .  $\square$

*Remark 2.9.* Theorem 2.8 demonstrates that if the subsystem can be solved exactly, i.e.,  $\{\tilde{\varepsilon}_k\}$  and  $\{\tilde{\eta}_k\}$  being equal to zero, the practical GADI-HS and the GADI-HS have the same convergent speed. Further, the convergent speed of the GADI-HS (the practical GADI-HS) method is faster than that of the HSS (the IHSS) method when  $\rho(T(\alpha, \omega)) < \rho(M(\alpha))$  according to Theorem 2.5.

To guarantee the convergence of the practical GADI-HS method in Theorem 2.8, it is sufficient to take  $\tilde{\varepsilon}_k$  and  $\tilde{\eta}_k$  such that the conditions of Lemma 2.7 are satisfied. Similar to [4], we can offer a feasible way to choose  $\tilde{\varepsilon}_k$  and  $\tilde{\eta}_k$  below.

**THEOREM 2.10.** *Let the assumptions of [Lemma 2.7](#) be met. Assume that sequences  $\{\tau_1(k)\}$  and  $\{\tau_2(k)\}$  are both nondecreasing and positive satisfying*

$$\tau_1(k) \leq 1, \quad \tau_2(k) \leq 1, \quad \limsup_{k \rightarrow \infty} \tau_1(k) = \limsup_{k \rightarrow \infty} \tau_2(k) = +\infty.$$

*Suppose that  $\mu_1$  and  $\mu_2$  are real constants in the interval  $(0, 1)$  satisfying*

$$\tilde{\varepsilon}_k \leq c_1 \mu_1^{\tau_1(k)}, \quad \tilde{\eta}_k \leq c_2 \mu_2^{\tau_2(k)}, \quad k = 0, 1, 2,$$

*where  $c_1$  and  $c_2$  are nonnegative constants. Then*

$$\|\tilde{x}^{(k+1)} - \tilde{x}^*\|_{M_2} \leq \sqrt{\rho(T(\alpha, \omega)) + \psi \theta_1 \mu^{\tau(k)}} \|\tilde{x}^{(k)} - \tilde{x}^*\|_{M_2}, \quad k = 0, 1, 2,$$

*where  $\tau(k) = \min\{\tau_1(k), \tau_2(k)\}$ ,  $\mu = \max\{\mu_1, \mu_2\}$ ,  $\psi = \max\left\{\sqrt{\gamma c_1 c_2}, \frac{c_1 \gamma + \theta_2 c_1 + c_2 \gamma}{2\sqrt{\rho(T(\alpha, \omega))}}\right\}$  with  $\gamma$  and  $\theta_2$  being defined in [Theorem 2.8](#). In particular, we have*

$$\limsup_{k \rightarrow \infty} \frac{\|\tilde{x}^{(k+1)} - \tilde{x}^*\|_{M_2}}{\|\tilde{x}^{(k)} - \tilde{x}^*\|_{M_2}} = \rho(T(\alpha, \omega)).$$

*Proof.* From [Theorem 2.8](#), we obtain

$$\begin{aligned} \|\tilde{x}^{(k+1)} - \tilde{x}^*\|_{M_2} &\leq (\rho(T(\alpha, \omega)) + \theta_1 \tilde{\varepsilon}_k (\gamma + \theta_2 + \theta_1 \gamma \tilde{\eta}_k) + \theta_1 \gamma \tilde{\eta}_k) \|\tilde{x}^{(k)} - \tilde{x}^*\|_{M_2} \\ &\leq (\rho(T(\alpha, \omega)) + \theta_1 c_1 \mu_1^{\tau_1(k)} (\gamma + \theta_2 + \theta_1 \gamma c_2 \mu_2^{\tau_2(k)}) + \theta_1 \gamma c_2 \mu_2^{\tau_2(k)}) \|\tilde{x}^{(k)} - \tilde{x}^*\|_{M_2} \\ &\leq (\rho(T(\alpha, \omega)) + \theta_1 c_1 \mu^{\tau(k)} (\gamma + \theta_2 + \theta_1 \gamma c_2 \mu^{\tau(k)}) + \theta_1 \gamma c_2 \mu^{\tau(k)}) \|\tilde{x}^{(k)} - \tilde{x}^*\|_{M_2} \\ &= (\rho(T(\alpha, \omega)) + (c_1 \gamma + \theta_2 c_1 + \gamma c_2) \theta_1 \mu^{\tau(k)} + \theta_1^2 \gamma c_1 c_2 \mu^{2\tau(k)}) \|\tilde{x}^{(k)} - \tilde{x}^*\|_{M_2} \\ &\leq (\rho(T(\alpha, \omega)) + 2\psi \sqrt{\rho(T(\alpha, \omega))} \theta_1 \mu^{\tau(k)} + \psi^2 \theta_1^2 \mu^{2\tau(k)}) \|\tilde{x}^{(k)} - \tilde{x}^*\|_{M_2} \\ &= (\sqrt{\rho(T(\alpha, \omega))} + \psi \theta_1 \mu^{\tau(k)})^2 \|\tilde{x}^{(k)} - \tilde{x}^*\|_{M_2}. \end{aligned}$$

It immediately holds that □

$$\limsup_{k \rightarrow \infty} \frac{\|\tilde{x}^{(k+1)} - \tilde{x}^*\|_{M_2}}{\|\tilde{x}^{(k)} - \tilde{x}^*\|_{M_2}} = \rho(T(\alpha, \omega)).$$

**2.4. GADI-AB scheme for linear matrix equations.** In this section, we apply the GADI framework to solve the matrix equation. We use a representative example, i.e., the continuous Sylvester equation, which has been widely used in control theory and numerical PDEs (see [\[15, 24, 26\]](#) and the references therein), to demonstrate the implementation. Concretely, the continuous Sylvester equation can be written as

$$(2.22) \quad AX + XB = C,$$

where  $A \in \mathbb{C}^{m \times m}$ ,  $B \in \mathbb{C}^{n \times n}$ , and  $C \in \mathbb{C}^{m \times n}$  are sparse matrices, and  $X \in \mathbb{C}^{m \times n}$  is the unknown matrix. Assume that  $A$  and  $B$  are positive semidefinite, at least one of them is positive definite, and at least one of them is non-Hermitian. Apparently, under these assumptions, the continuous Sylvester equation [\(2.22\)](#) has a unique solution.

Applying the GADI framework to [\(2.22\)](#) and replacing splitting matrices  $M$  and  $N$  in [\(2.1\)](#) with matrices  $A$  and  $B$  in [\(2.22\)](#), we obtain the GADI-AB method. Given

an initial guess  $X^{(0)}$  and  $\hat{\alpha} > 0$ ,  $\hat{\omega} \geq 0$ , the GADI-AB framework is

$$(2.23) \quad \begin{cases} (\hat{\alpha}I + A)X^{(k+\frac{1}{2})} = X^{(k)}(\hat{\alpha}I - B) + C, \\ X^{(k+1)}(\hat{\alpha}I + B) = X^{(k)}(B - (1 - \hat{\omega})\hat{\alpha}I) + (2 - \hat{\omega})\hat{\alpha}X^{(k+\frac{1}{2})}, \end{cases}$$

where  $k = 0, 1, \dots$ . The following theorem gives the convergence result of the GADI-AB method.

**THEOREM 2.11.** *Let  $A \in \mathbb{C}^{n \times n}$  be positive definite matrix and  $B \in \mathbb{C}^{n \times n}$  be semipositive definite matrix. Then the GADI-AB method (2.23) is convergent to the unique solution  $X^*$  of the continuous Sylvester equation (2.22) for any  $\hat{\alpha} > 0$  and  $\hat{\omega} \in [0, 2)$ .*

*Proof.* It is evident that the GADI-AB method satisfies the conditions of [Theorem 2.3](#) according to the properties of  $A$  and  $B$ . Therefore, the GADI-AB method converges to the unique solution  $x^*$  of (2.22).  $\square$

**3. Parameter selection.** The effectiveness of the ADI schemes is sensitive to the splitting parameters. How to efficiently and accurately obtain relatively optimal parameters in splitting methods is still a challenge. A common approach is traversing parameters within an interval by amounts of numerical experiments. The traversing method can obtain relatively accurate optimal parameters; however, it consumes much repetitive computational amount [3, 15, 26]. Another approach is using theoretical analysis to estimate the splitting parameters [3, 4, 19, 24]. However, the theoretical method is available on a case-by-case basis, and the effectiveness relies heavily on the theoretical estimate. In this section, we provide a data-driven parameter selection method, the GPR approach based on the Bayesian inference, which can efficiently obtain accurate splitting parameters. It is emphasized that the proposed GPR method can be available to the GADI framework and other splitting schemes. As a comparison, we present a theoretical method of selecting splitting parameters for the GADI-HS method as well. It also should be pointed out that the theoretical method is a case-by-case basis. For the practical GADI-HS and GADI-AB methods, there has been no theory to estimate splitting parameters.

**3.1. Gaussian process regression.** In this section, the GPR method is proposed to estimate the optimal parameters of the GADI framework. GPR is a new regression method, which has developed rapidly during the last two decades. Therefore, the GPR method has wide applications and has become a heated issue in machine learning [13, 20]. It has lots of advantages such as being easy to implement, flexible to nonparameter infer, and adaptive to obtaining hyperparameters. The relatively optimal ADI parameters might be dependent on other quantities, such as the eigenvalues of the coefficient matrices. In practical implementation, we only require a user-friendly mapping to obtain the relatively optimal ADI parameters. The scale of linear systems is one of the most readily available quantities. Therefore, we choose to learn the mapping between the input dimension  $n$  and the output parameter  $\alpha$ .

### 3.1.1. GPR prediction.

**DEFINITION 3.1.** *The Gaussian process (GP) is a collection of random variables which follows the joint Gaussian distribution.*

Assume that we have a training set  $D = \{(n_i, \alpha_i) \mid i = 1, 2, \dots, d\} := \{\mathbf{n}, \boldsymbol{\alpha}\}$ , where  $(n_i, \alpha_i)$  is an input-output pair,  $n_i$  is the dimension of the iterative matrix, and  $\alpha_i$  is the splitting parameter in the GADI framework. If  $\alpha_i$  with respect to  $n_i$

obeys the GP, then  $f(\mathbf{n}) = [f(n_1), f(n_2), \dots, f(n_d)]$  obeys the  $d$ -dimensional Gaussian distribution (GD)

$$\begin{bmatrix} f(n_1) \\ \vdots \\ f(n_d) \end{bmatrix} \sim N \left( \begin{bmatrix} \mu(n_1) \\ \vdots \\ \mu(n_d) \end{bmatrix}, \begin{bmatrix} k(n_1, n_1) & \cdots & k(n_1, n_d) \\ \vdots & \ddots & \vdots \\ k(n_d, n_1) & \cdots & k(n_d, n_d) \end{bmatrix} \right).$$

Evidently, GP is determined by its mean function  $\mu(n)$  and covariance function  $k(n, n)$ . This is a natural generalization of the GD whose mean and covariance are a vector and a matrix, respectively. We can rewrite the above GP as

$$f(\mathbf{n}) \sim GP(\mu(\mathbf{n}), K(\mathbf{n}, \mathbf{n}')),$$

where  $\mathbf{n}, \mathbf{n}'$  are any two random variables in the input set  $\mathbf{n}$ . We usually set the mean function to be zero.

The task of the GPR method is to learn a mapping relationship between the input set  $\mathbf{n}$  and output set  $\boldsymbol{\alpha}$ , i.e.,  $f(\mathbf{n}) : \mathbb{N} \mapsto \mathbb{R}$ , and infer the most possible output value  $\alpha_* = f(n_*)$  given the new test point  $n_*$ . In an actual linear regression problem, we consider the model as

$$\alpha = f(\mathbf{n}) + \eta,$$

where  $\alpha$  is the observed value polluted by additivity noise  $\eta$  to prevent the singularity of generated matrix. Further, assume that  $\eta$  follows a GD with zero mean and variance  $\sigma^2$ , i.e.,  $\eta \sim N(0, \sigma^2)$ . The desirable range of  $\sigma$  is  $[10^{-6}, 10^{-2}]$ . In this work we take  $\sigma = 10^{-4}$  in numerical calculations.

Therefore, the prior distribution of observed value  $\boldsymbol{\alpha}$  becomes

$$\boldsymbol{\alpha} \sim N(\boldsymbol{\mu}_\alpha(\mathbf{n}), K(\mathbf{n}, \mathbf{n}) + \sigma^2 I_d).$$

The joint prior distribution of observed value  $\boldsymbol{\alpha}$  and prediction  $\boldsymbol{\alpha}_*$  becomes

$$\begin{bmatrix} \boldsymbol{\alpha} \\ \boldsymbol{\alpha}_* \end{bmatrix} \sim N \left( \begin{bmatrix} \boldsymbol{\mu}_\alpha \\ \boldsymbol{\mu}_{\alpha_*} \end{bmatrix}, \begin{bmatrix} K(\mathbf{n}, \mathbf{n}) + \sigma^2 I_d & K(\mathbf{n}, \mathbf{n}_*) \\ K(\mathbf{n}_*, \mathbf{n}) & K(\mathbf{n}_*, \mathbf{n}_*) \end{bmatrix} \right),$$

where  $I_d$  is a  $d$ -order identity matrix, and  $K(\mathbf{n}, \mathbf{n}) = (k_{ij})$  is a symmetric positive definite covariance matrix with  $k_{ij} = k(n_i, n_j)$ .  $K(\mathbf{n}, \mathbf{n}_*)$  is a symmetric covariance matrix between the training set  $\mathbf{n}$  and test set  $\mathbf{n}_*$ .

Using the Bayesian formula

$$(3.1) \quad p(\boldsymbol{\alpha}_* | \boldsymbol{\alpha}) = \frac{p(\boldsymbol{\alpha} | \boldsymbol{\alpha}_*) p(\boldsymbol{\alpha}_*)}{p(\boldsymbol{\alpha})},$$

the joint posterior distribution of prediction is

$$(3.2) \quad \boldsymbol{\alpha}_* | \mathbf{n}, \boldsymbol{\alpha}, \mathbf{n}_* \sim N(\boldsymbol{\mu}_*, \boldsymbol{\sigma}_*^2),$$

where

$$\begin{aligned} \boldsymbol{\mu}_* &= K(\mathbf{n}_*, \mathbf{n}) [K(\mathbf{n}, \mathbf{n}) + \sigma^2 I_d]^{-1} (\boldsymbol{\alpha} - \boldsymbol{\mu}_\alpha) + \boldsymbol{\mu}_{\alpha_*}, \\ \boldsymbol{\sigma}_*^2 &= K(\mathbf{n}_*, \mathbf{n}_*) - K(\mathbf{n}_*, \mathbf{n}) [K(\mathbf{n}, \mathbf{n}) + \sigma^2 I_d]^{-1} K(\mathbf{n}, \mathbf{n}_*). \end{aligned}$$

The derivation procedure can refer to [20]. For the output  $\alpha_*$  in the test set, one can use the mean value of the above GP as its estimated value, i.e.,  $\hat{\alpha}_* = \mu_*$ .

The kernel function is the key of the GPR method, which generates the covariance matrix to measure the distance between any two input variables. When the distance is closer, the correlation of the corresponding output variables is greater. Therefore, we need to choose or construct the kernel function according to actual requirements. The most commonly used kernel functions include the radial basis function, the rational quadratic kernel function, the exponential kernel function, and the periodic kernel function. For more kernel functions refer to [20]. In this work, we choose the exponential kernel function

$$(3.3) \quad k(x, y) = \sigma_f^2 \exp\left(\frac{-\|x - y\|}{2l^2}\right),$$

where  $\theta = \{l, \sigma_f\}$  is the hyperparameter,  $\|x - y\| = \sqrt{\sum_i (x_i - y_i)^2}$ . The optimal hyperparameter is determined by maximizing the marginal-log likelihood function  $p(y|x, \theta)$ , i.e.,

$$(3.4) \quad L = \log p(y|x, \theta) = -\frac{1}{2}y^T[K + \sigma^2 I_d]^{-1}y - \frac{1}{2} \log \|K + \sigma^2 I_d\| - \frac{n}{2} \log 2\pi.$$

Maximizing  $L$  corresponds to an unconstrained nonlinear optimization problem. We use the L-BFGS method to address it, which costs little time.

**3.1.2. The implementation of GPR.** Since the GPR results from probability distribution, the regression and prediction have a specific confidence interval. The confidence interval is defined as follows,

**DEFINITION 3.2** (confidence interval). *Suppose a data set  $x_1, \dots, x_n$  is given, modeled as the realization of random variables  $X_1, \dots, X_n$ . Let  $\alpha$  be the parameter of interest and  $\gamma$  be a number between 0 and 1. If there exist sample statistics  $L_n = g(X_1, \dots, X_n)$  and  $U_n = h(X_1, \dots, X_n)$  such that*

$$P(L_n < \theta < U_n) = \gamma$$

*for every value of  $\alpha$ , then  $(l_n, u_n)$ , where  $l_n = g(x_1, \dots, x_n)$  and  $u_n = h(x_1, \dots, x_n)$ , is called a  $100\gamma$  confidence interval for  $\alpha$ . The number  $\gamma$  is called the confidence level.*

The number  $l_n$  ( $u_n$ ) is called a  $100\gamma\%$  lower (upper) confidence bound for parameter  $\alpha$ .

**Figure 1** summarizes the process of GPR. Here, the confidence interval denotes the area of the normal distribution of mean  $\mu$  and standard deviation  $\sigma$  falling in the interval  $(\mu - 1.96\sqrt{\text{diag}(\sigma)}, \mu + 1.96\sqrt{\text{diag}(\sigma)})$  accounts for about 95%. Ninety-five percent of the sample means selected from a population will be within 1.96 standard deviations of the population mean  $\mu$ . From **Figure 1**, it can be seen that the GPR method has established a mapping between the matrix scale  $n$  and the parameter  $\alpha$ . We input known data to train an inference model and then predict the unknown parameters. The known relatively optimal parameters in the training data set come from small-scale linear systems, while the unknown parameter belongs to that of large linear systems. To predict the parameter more accurately and extensively, we also put the predicted data into the training set to form the retraining set. Subsequently, we use the latest model to predict the parameters of much larger linear systems.

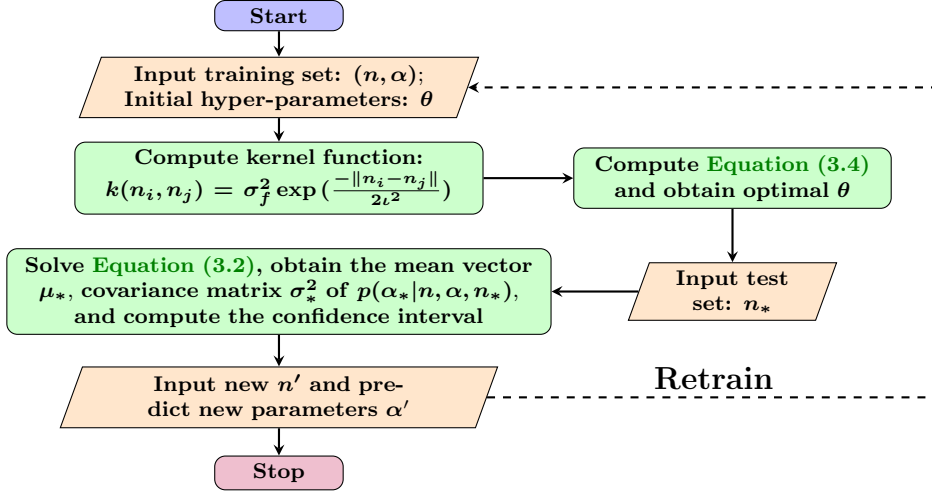


Fig. 1: Flow chart of GPR parameters prediction.

**3.2. Quasi-optimal parameter of GADI-HS.** In this section, we offer a theoretical way to select the quasi-optimal parameter of the GADI-HS method. We first estimate an upper bound of the iterative matrix spectral radius of the GADI-HS method.

LEMMA 3.3. *Let  $A \in \mathbb{C}^{n \times n}$  be a positive definite matrix,  $H$  and  $S$  defined by (2.6) be its Hermitian and skew-Hermitian parts,  $\alpha$  be a positive constant, and  $\omega \in [0, 2)$ . Then the spectral radius  $\rho(T(\alpha, \omega))$  is bounded by*

$$(3.5) \quad \rho(T(\alpha, \omega)) \leq \frac{\alpha^2 + \alpha|1 - \omega|\|A\|_2 + \lambda_{max}\sigma_{max}}{\alpha(\alpha + \lambda_{min})} = \delta(\alpha^*, \omega^*),$$

where  $T(\alpha, \omega)$  is defined in (2.8),  $\sigma_{max}$  is the maximum singular value of  $S$ , and  $\lambda_{min}$  and  $\lambda_{max}$  are the minimum and maximum eigenvalues of  $H$ , respectively.

*Proof.* The proof is in Appendix A.2. □

LEMMA 3.4 ([4]). *Let  $A \in \mathbb{C}^{n \times n}$  be a positive definite matrix,  $H$  and  $S$  defined by (2.6) be its Hermitian and skew-Hermitian parts, and  $\alpha$  be a positive constant. Then the quasi-optimal parameter of the HSS iterative method is*

$$\alpha^* = \sqrt{\lambda_{min}\lambda_{max}}, \quad \text{and} \quad \sigma(\alpha^*) = \frac{\sqrt{\lambda_{max} - \sqrt{\lambda_{min}}}}{\sqrt{\lambda_{max} + \sqrt{\lambda_{min}}}} = \frac{\sqrt{\kappa(H)} - 1}{\sqrt{\kappa(H)} + 1},$$

where  $\lambda_{min}$  and  $\lambda_{max}$  are the minimum and maximum eigenvalues of  $H$ , and  $\kappa(H)$  is the spectral condition number of  $H$ .

THEOREM 3.5 (the quasi-optimal parameter of GADI-HS). *Let  $A \in \mathbb{C}^{n \times n}$  be a positive definite matrix,  $H$  and  $S$  defined by (2.6) be its Hermitian and skew-Hermitian parts,  $\alpha > 0$ , and  $\omega \in [0, 2)$ , and  $\lambda_k$  be the eigenvalue of the iterative matrix  $M(\alpha)$ . For the quasi-optimal parameter  $(\alpha^*, \omega^*)$  of the GADI-HS method, we have the following conclusions.*

(i) When  $|\lambda_k|^2 \leq a$ , then

$$\omega^* = 0, \quad \alpha^* = \sqrt{\lambda_{\min}\lambda_{\max}}, \quad \text{and} \quad \delta(\alpha^*, \omega^*) = \sigma(\alpha^*),$$

where  $\sigma(\alpha^*)$  is defined in [Lemma 3.4](#), and  $\lambda_{\min}$  and  $\lambda_{\max}$  are the minimum and maximum eigenvalues of  $H$ , respectively.

(ii) When  $a < |\lambda_k|^2$  and  $0 < \omega < \frac{4a^2 - 4a + 4b^2}{(1-a)^2 + b^2}$ , then

$$\omega^* = 1, \quad \alpha^* = \frac{p + \sqrt{p^2 + \lambda_{\min}^2 p}}{\lambda_{\min}},$$

and

$$\delta(\alpha^*, \omega^*) = \frac{2p^2 + 2\lambda_{\min}^2 p + 2p\sqrt{p^2 + \lambda_{\min}^2 p}}{2p^2 + 2\lambda_{\min}^2 p + 2p\sqrt{p^2 + \lambda_{\min}^2 p} + \lambda_{\min}^2 \sqrt{p^2 + \lambda_{\min}^2 p}} < 1,$$

where  $p = \lambda_{\max}\sigma_{\max}$ ,  $\sigma_{\max}$  is the maximum singular value of  $S$ .

*Proof.* The proof is in [Appendix A.3](#).  $\square$

*Remark 3.6.* From [Lemma 3.3](#), it implies that the bound of  $\rho(T(\alpha, \omega))$  is related to the singular value of  $S$  and the eigenvalue of  $H$ . However, directly estimating  $\alpha$  for the GADI-HS method is difficult in actual implementation. Here we minimize the upper bound to obtain a quasi-optimal  $\alpha$  but not the optimal  $\alpha$ .

**4. Numerical experiments.** In this section, we present extensive numerical examples to show the power of the GADI framework and the GPR method. Concretely, we take a 3D convection-diffusion equation, 2D parabolic equation (see [Appendix A.4](#)), and continuous Sylvester equation as examples to demonstrate the efficiency of GADI-HS, practical GADI-HS, and GADI-AB. All computations are carried out using MATLAB 2018a on a Mac laptop with a 2.3 GHz CPU Intel Core i5 and 8G memory. We employ the GPR method to predict the optimal splitting parameters for the GADI framework. The whole procedure of GPR prediction only takes about 1 ~ 2 seconds in the offline training. From numerical calculations, we find that  $\omega$  is insensitive to the order of linear systems. Thus we can obtain the relatively optimal  $\omega$  in small-scale linear systems, then apply the GPR method to predict the relatively optimal  $\alpha$ .

**4.1. Three-dimensional convection-diffusion equation.** Consider the following 3D convection-diffusion equation:

$$(4.1) \quad -(u_{x_1 x_1} + u_{x_2 x_2} + u_{x_3 x_3}) + (u_{x_1} + u_{x_2} + u_{x_3}) = f(x_1, x_2, x_3)$$

on the unit cube  $\Omega = [0, 1] \times [0, 1] \times [0, 1]$  with Dirichlet-type boundary condition [\[4\]](#). We use the centered difference method to discretize the convective-diffusion equation [\(4.1\)](#), and obtain the linear system  $Ax = b$ . The coefficient matrix is

$$(4.2) \quad A = T_1 \otimes I \otimes I + I \otimes T_2 \otimes I + I \otimes I \otimes T_3,$$

where  $T_1$ ,  $T_2$  and  $T_3$  are tridiagonal matrices.  $T_1 = \text{Tridiag}(t_2, t_1, t_3)$ ,  $T_2 = T_3 = \text{Tridiag}(t_2, 0, t_3)$ ,  $t_1 = 6$ ,  $t_2 = -1 - \beta$ ,  $t_3 = -1 + \beta$ ,  $\beta = 1/(2n + 2)$ .  $n$  is the degree of freedom along each dimension,  $x \in \mathbb{R}^{n^3}$  is the unknown vector of discretizing  $u(x_1, x_2, x_3)$ .  $b \in \mathbb{R}^{n^3}$  is the discretization vector of  $f(x_1, x_2, x_3)$  which is determined



by choosing the exact solution  $x_e = (1, 1, \dots, 1)^T$ . All tests are started with the zero vector. All iterative methods are terminated if the relative residual error satisfies

$$(4.3) \quad \text{RES} = \|r^{(k)}\|_2 / \|r^{(0)}\|_2 \leq 10^{-6},$$

where  $r^{(k)} = b - Ax^{(k)}$  is the  $k$ -step residual.

**4.1.1. A comparison of GADI-HS and HSS.** First, we examine the efficiency of the GADI framework in solving the above linear algebra equation. Concretely, we apply the HSS and GADI-HS methods to solve  $Ax = b$ . The parameters in the HSS and GADI-HS methods are obtained from [Lemma 3.4](#) and [Theorem 3.5](#), respectively. [Table 2](#) shows the numerical results, where ‘‘IT’’ and ‘‘CPU’’ denote the required iterations and the CPU time (in seconds), respectively.

Table 2: Results of the HSS and the GADI-HS methods for solving 3D convection-diffusion equation with theoretical quasi-optimal splitting parameters.

$n^3$	HSS			GADI-HS		
	$\alpha_q$	IT	CPU(s)	$(\alpha_q, \omega_q)$	IT	CPU(s)
$8^3(512)$	2.0521	37	0.03	(0.6208,1.0)	29	0.02
$12^3(1728)$	1.4359	52	0.13	(0.4468,1.0)	39	0.06
$16^3(4096)$	1.1025	66	1.87	(0.3465,1.0)	48	0.99
$20^3(8000)$	0.8943	79	9.17	(0.2823,1.0)	56	4.82
$24^3(13824)$	0.7520	92	30.89	(0.2380,1.0)	65	16.69

From [Table 2](#), one can find that the GADI-HS method spends about half the CPU time compared with the HSS method. It is consistent with [Theorem 3.5](#), which shows the convergence speed of the GADI-HS scheme is faster than the HSS method. These results demonstrate that the GADI-HS scheme derived from the new GADI framework accelerates the convergence speed in solving [\(4.1\)](#). However, we can find that both methods cost much time for relatively large linear systems.

**4.1.2. Applying the Practical GADI-HS method.** Next, we use the practical GADI-HS ([Algorithm 2.1](#)) and the IHSS methods to solve much larger linear systems. Meanwhile, we employ the GPR method to predict the splitting parameters in the practical GADI-HS method. The inner subsystems [\(2.12\)](#) and [\(2.13\)](#) are solved by the CG and the CGNE methods, respectively. The inner iteration is terminated if residuals satisfy

$$\|p^{(k)}\|_2 \leq 1 \times 10^{-\delta_H} \|r^{(k)}\|_2, \quad \|q^{(k)}\|_2 \leq 1 \times 10^{-\delta_S} \|r^{(k+\frac{1}{2})}\|_2,$$

where  $\delta_H$  and  $\delta_S$  are controllable tolerances in the inner iteration to balance the Hermitian and skew-Hermitian parts in the linear subproblems. In these tests, we set  $\delta_H = \delta_S = 2$ .

There has been no theoretical approach to estimate splitting parameters for inexact ADI methods, such as the practical GADI-HS and the IHSS schemes. For the IHSS method, the splitting parameters can be obtained by the traversing method, be determined experimentally [\[4, 7, 24\]](#), or obtained directly by the GPR method as presented in [subsection 4.1.3](#). Here, we use the traversing method to obtain the relatively optimal parameter  $\alpha^*$  of IHSS in the traversing interval  $(0, 3]$  with a step size of 0.01. We use the GPR method to predict the splitting parameter  $\alpha$  for the practical GADI-HS scheme. [Table 3](#) gives the training, test, and retrained data sets.  $\alpha$  in the

training data set of the GPR approach is produced by traversing parameters as the IHSS method does, but for small-scale linear systems,  $n$  from 2 to 66 with different step size  $\Delta n$ . The matrix order  $n$  in the test data set is from 1 to 120 with  $\Delta n = 1$ , while  $n$  in the retrained data set is from 70 to 120 with  $\Delta n = 6$ . Figure 2 shows the optimal parameter regression and prediction processes for the practical GADI-HS method. From Figure 2, we can find that adding predicted points into the training set which forms the retrained set can shrink the confidence interval. This improves the prediction accuracy and strengthens the generalization ability of the regression model. Since  $\omega$  is insensitive to the scale of matrix in the practical GADI-HS, we obtain the optimal  $\omega_p = 1.9$  by the traversing method for small-scale systems.

Table 3: The training, test, and retrained data sets of the practical GADI-HS method in GPR algorithm.

Training set	$n : 2 \sim 10, \Delta n = 2$ $n : 12 \sim 20, \Delta n = 4$ $n : 28 \sim 44, \Delta n = 8$ $n : 56 \sim 66, \Delta n = 10$
Test set	$n : 1 \sim 120, \Delta n = 1$
Retrained set	$n : 70 \sim 120, \Delta n = 6$

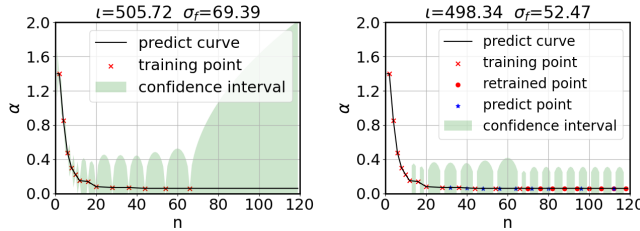


Fig. 2: The regression curve of  $\alpha$  against  $n$  for the practical GADI-HS method.

Table 4 presents the numerical results obtained by the IHSS and practical GADI-HS methods for different scale discretization systems.  $IT_{CG}$  and  $IT_{CGNE}$  denote the iterations for solving subsystems in inexact methods. These results show that the IHSS method can solve relatively large linear systems ( $n^3$  from  $32^3$  to  $64^3$ ) with less CPU time than the HSS algorithm does when the relatively optimal parameter  $\alpha^*$  is used. However, obtaining  $\alpha^*$  in the IHSS costs lots of traversal time, as shown in the last column in Table 4. For example, when  $n = 64^3$ , the traversal time of the IHSS method is more than 7000 seconds. As  $n$  further increases, the traversal times would become unaffordable. Meanwhile, it should be emphasized that the efficiency of ADI schemes is very sensitive to the accuracy of splitting parameter  $\alpha$ . As Figure 3 shows, when  $n = 64^3$ , the IT still changes as the traversing step size becomes  $10^{-4}$ . However, it will cost much more traversing CPU time if one uses a smaller step size to find a more optimal  $\alpha$ . Therefore, obtaining an efficient performance of the IHSS scheme may require undergoing very expensive computation by finding a relatively optimal splitting parameter  $\alpha$ .

Compared with the IHSS method, the practical GADI-HS scheme is much more efficient in combination with the GPR approach. The GPR method can predict a

Table 4: Results of the IHSS method ( $\alpha^*$  obtained by traversing interval  $(0, 3]$  with a step size of 0.01) and the practical GADI-HS method (relatively optimal parameters  $(\alpha_p, \omega_p)$  obtained by the GPR algorithm) for solving 3D convection-diffusion equation.

Method	$n^3$	$\alpha^*$	IT ( $IT_{CG}, IT_{CGNE}$ )	CPU (s)	Traversal CPU(s)
IHSS	$32^3(32768)$	0.93	185 (4.19, 1.00)	0.83	477.77
	$48^3(110592)$	0.90	369 (4.02, 1.00)	4.44	2239.66
	$64^3(261144)$	0.89	612 (3.95, 1.00)	20.43	7025.53
	$n^3$	$(\alpha_p, \omega_p)$	IT ( $IT_{CG}, IT_{CGNE}$ )	CPU (s)	Traversal CPU(s)
Practical GADI-HS	$32^3(32768)$	(0.0699, 1.9)	23 (23.35, 2.00)	0.26	0
	$48^3(110592)$	(0.0599, 1.9)	33 (21.45, 1.21)	1.09	0
	$64^3(261144)$	(0.0599, 1.9)	54 (22.72, 1.07)	4.21	0
	$96^3(884736)$	(0.0596, 1.9)	110 (19.75, 1.00)	32.48	0
	$128^3(2097152)$	(0.0595, 1.9)	186 (13.92, 1.00)	113.82	0
	$216^3(10077696)$	(0.0595, 1.9)	478 (12.64, 1.00)	1539.48	0

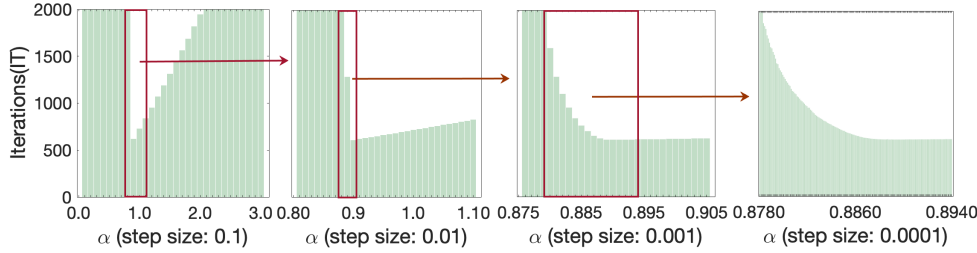


Fig. 3: When  $n = 64^3$ , the variation of the iterations (IT) of the IHSS method on the traversal parameter  $\alpha$  of different step size.

relatively optimal  $\alpha$  through training a mapping from  $n$  to  $\alpha$ . The small set of training data is obtained by the offline computation for small-scale systems. The learned mapping can directly predict a relatively optimal splitting parameter  $\alpha$  for large systems without any extra computational amount, as Figure 2 shows. Therefore in the practical (online) computation, the practical GADI-HS scheme can obtain the solution with an efficient one-shot computation and does not consume traversal CPU time anymore. And with accurate  $\alpha$ , the practical GADI-HS method can efficiently solve large linear systems, even of more than ten million orders. As an example, Figure 4 plots the convergent curve of IHSS and practical GADI-HS when  $n^3 = 64^3$ .

Meanwhile, from Tables 3 and 4, one can find that the maximum order in the training set is  $66^3(287496)$ , while the order of matrix in the test set can reach the level of ten million ( $216^3$ ). It means that the scale of the predictable  $n$  can attain about 35 times. It means that the order of matrix in the given training set is  $n$ , and the prediction ability of the GPR method can reach a scale of  $35n$ . These results demonstrate that the GPR model has a high generalization capability.

We further plot the CPU cost of the HSS, IHSS, GADI-HS, and practical GADI-HS methods as  $n^3$  increases from  $8^3$  to  $216^3$  as shown in Figure 5. The concrete CPU times can be found in Tables 2 and 4. For the IHSS method, Figure 5 only presents its best performance in solving (4.1) and ignores the CPU time of finding  $\alpha^*$ . From

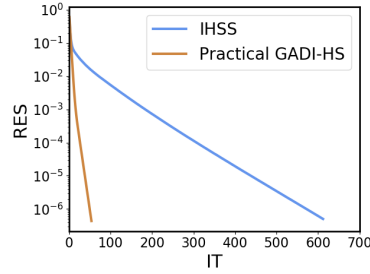


Fig. 4: The convergent curves of IHSS and practical GADI-HS when  $n^3 = 64^3$  for solving 3D convection-diffusion equation.

these results, one can find that the practical GADI-HS method costs less CPU time. For example, when  $n^3 = 128^3$ , the IHSS method (594.28 seconds) spends about five times CPU time more than the practical GADI-HS scheme (113.82 seconds) does. It should be emphasized that the IHSS method costs much traversal time of over 10000 seconds to obtain a good performance (traversing  $\alpha^*$  in  $[0.8, 0.9]$  with a step size of 0.01), while the practical GADI-HS method does not have traversing time due to the GPR method. If one considers all costs, the practical GADI-HS saves over 100 times the computational cost for the case of  $n^3 = 128^3$ .

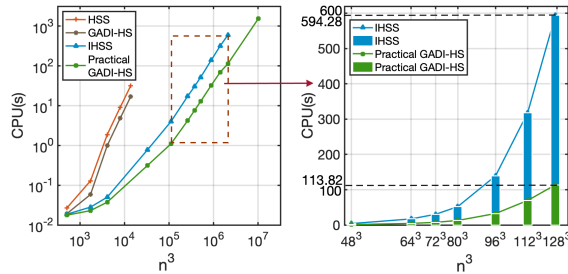


Fig. 5: Left: The CPU time of HSS, IHSS, GADI-HS, and practical GADI-HS methods for different  $n$ . Right: The comparison of CPU time between IHSS and practical GADI-HS methods for  $n$  from 48 to 128.

Moreover, we compare the practical GADI-HS method with the GMRES, preconditioned GMRES, and iLU methods for solving the 3D convection-diffusion equation, as Table 5 shows. It can be seen that the practical GADI-HS method is more efficient than the GMRES and iLU methods, and has similar performance with some efficient preconditioned GMRES, such as the Toeplitz preconditioner proposed by Strang [21]. It should be stressed that the GADI framework is the first work to greatly increase the performance of splitting methods in solving large sparse linear systems. It has enormous potential to further promote the performance of the GADI methods corresponding the structure of linear systems.

**4.1.3. Predicting the optimal splitting parameter of the IHSS method by the GPR.** Here we apply the GPR method to predict the optimal splitting

Table 5: A comparison of the practical GADI-HS, GMRES, preconditioned GMRES, and iLU methods for solving 3D convection-diffusion equation.

$n^3$	Practical GADI-HS		GMRES		Preconditioned GMRES		iLU
	IT	CPU(s)	IT	CPU(s)	IT	CPU(s)	CPU(s)
$32^3$ (32768)	23	0.26	97	0.46	17	0.30	32.56
$48^3$ (110592)	33	1.09	141	1.91	24	1.22	1166
$64^3$ (262144)	54	4.21	184	7.44	35	4.26	>5000
$96^3$ (884736)	110	32.48	265	75.25	57	26.13	

parameter of the IHSS scheme. The training, test, and retrained data sets are given in Table 6. The implementation of the GPR method is the same as the Subsection 4.1.2. Figure 6 gives the inference curve of the GPR.

Table 6: The training, test, and retrained sets of the GPR approach for predicting the optimal splitting parameter of the IHSS method in solving 3D convection-diffusion equation.

Training set	$n : 2 \sim 10, \Delta n = 2$ $n : 12 \sim 20, \Delta n = 4$ $n : 24 \sim 48, \Delta n = 8$ $n : 64$
Test set	$n : 1 \sim 120, \Delta n = 1$
Retrained set	$n : 70 \sim 120, \Delta n = 6$

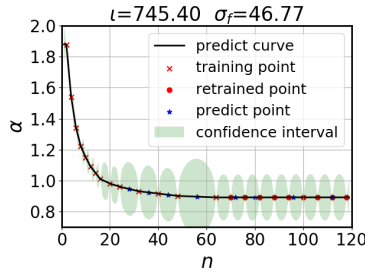


Fig. 6: The  $\alpha$  regression curve of the IHSS method.

Table 7 shows the prediction results and the performance of IHSS method. In Table 7, the second column is the optimal traversing parameter  $\alpha$  with step size 0.01, the third column is the predicted parameter  $\alpha^*$  obtained by the GPR, and the fourth (IT) and fifth (IT\*) columns are iteration steps corresponding to splitting parameters  $\alpha$  and  $\alpha^*$ , respectively. From Table 7, we can find that the GPR method can predict accurate splitting parameters which are consistent with the traversing method. As a result, the iteration steps IT and IT\* of the IHSS method are nearly the same for convergence. More significantly, when the dimension  $n^3$  of the linear system becomes large to  $112^3$ , the GPR method can predict more accurate splitting parameter which can promote the performance of the IHSS. These results demonstrate that the GPR can be applied to other ADI schemes.

Table 7: A performance comparison of traversing parameter  $\alpha$  and predicting parameter  $\alpha^*$  by the GPR in the IHSS method when solving 3D convection-diffusion equation.

$n^3$	$\alpha$	$\alpha^*$	IT	IT*
$28^3$ (21952)	0.94	0.9450	149	148
$36^3$ (46656)	0.92	0.9225	226	226
$44^3$ (85184)	0.91	0.9075	317	319
$56^3$ (175616)	0.90	0.8950	484	488
$72^3$ (373248)	0.89	0.8899	759	759
$80^3$ (512000)	0.89	0.8900	920	920
$96^3$ (884736)	0.89	0.8896	1284	1285
$112^3$ (1404928)	0.88	0.8884	1702	1682

*Remark 4.1.* Here, let us give a remark to show the reasonableness of using the dimension  $n$  as the input variable in the GRP method. Table 8 shows the relationship between the condition number and dimensional coefficient matrix  $A$  of the 3D convection-diffusion equation. It can be seen that the condition number of coefficient matrix  $A$  increases as the dimension  $n$  increases. This means that minimal or maximal eigenvalues of  $A$  are depend on  $n$ . The goal of GPR is to learn a mapping from a readily available quantity to the optimal splitting parameter in the GADI framework. The dimension  $n$  is the required quantity and can reflect some essential features of the coefficient matrix, such as eigenvalues. Thus, it is reasonable to choose  $n$  as the input variable.

Table 8: The condition number of  $A$  with different  $n$  when solving 3D convection-diffusion equation.

$n^3$	$8^3$	$16^3$	$32^3$	$48^3$	$64^3$
Condition number	53.0767	192.6712	727.6907	1.6079e+03	2.8294e+03

**4.2. The continuous Sylvester equation.** In this subsection, we consider the continuous Sylvester equation (2.22). The sparse matrices  $A$  and  $B$  have the following structure:

$$A = B = M + 2rN + \frac{100}{(n+1)^2}I,$$

where  $r$  is a parameter which controls Hermitian dominated or skew-Hermitian dominated of the matrix,  $M, N \in \mathbb{C}^{n \times n}$  are tridiagonal matrices  $M = \text{Tridiag}(-1, 2, -1)$ , and  $N = \text{Tridiag}(0.5, 0, -0.5)$ . We apply the HSS and the GADI-AB methods to solve (2.22) for  $r = 0.01, 0.1, \text{ and } 1$ , respectively. All iterative methods are started from zero matrix and stopped once the current residual norm satisfies  $\|R^{(k)}\|_F / \|R^{(0)}\|_F \leq 10^{-6}$ , where  $R^{(k)} = C - AX^{(k)} - X^{(k)}B$ .

Table 9 lists the simulation results of the HSS and GADI-AB methods. For the continuous Sylvester equation, the HSS and GADI-AB methods do not have theories to estimate relatively optimal splitting parameters. Here we can use the traversal approach to estimate the relatively optimal splitting parameters. The optimal parameter  $\alpha^*$  is obtained by traversing the interval  $(0, 3]$  with a step size of 0.01, while the optimal parameter  $\omega^*$  is obtained through traversing the interval  $[0, 2)$  with a step

Table 9: Results of the HSS and GADI-AB methods for solving the continuous Sylvester equation. The relatively optimal splitting parameter  $\alpha^*$  ( $\omega^*$ ) is obtained by traversing the interval  $(0, 3]$  ( $[0, 2)$ ) with a step size of 0.01 (0.1).

$n$	$r = 0.01$			HSS $r = 0.1$			$r = 1$		
	IT	CPU(s)	$\alpha^*$	IT	CPU(s)	$\alpha^*$	IT	CPU(s)	$\alpha^*$
16	23	0.0059	1.23	22	0.0051	1.28	14	0.0032	1.57
32	43	0.0307	0.64	41	0.0281	0.64	21	0.0146	1.07
64	83	0.3512	0.33	69	0.3053	0.32	31	0.1242	0.87
128	160	3.7057	0.17	112	2.6082	0.19	46	1.0632	0.74
256	312	42.9613	0.09	163	24.0084	0.14	68	10.3410	0.58

$n$	$r = 0.01$			GADI-AB $r = 0.1$			$r = 1$		
	IT	CPU(s)	$(\alpha^*, \omega^*)$	IT	CPU(s)	$(\alpha^*, \omega^*)$	IT	CPU(s)	$(\alpha^*, \omega^*)$
16	12	0.0001	(1.18,0.0)	12	0.0001	(1.18,0.0)	8	0.0001	(1.87,0.0)
32	22	0.0007	(0.62,0.0)	21	0.0007	(0.65,0.0)	12	0.0004	(1.28,0.1)
64	42	0.0038	(0.33,0.0)	38	0.0035	(0.36,0.0)	16	0.0011	(0.97,0.1)
128	81	0.0443	(0.17,0.0)	63	0.0370	(0.22,0.0)	21	0.0063	(0.76,0.1)
256	157	0.4499	(0.09,0.0)	90	0.2457	(0.15,0.0)	29	0.0605	(0.54,0.1)

size of 0.1. From Table 9, one can find that the GADI-AB method is much more efficient than the HSS method in terms of the IT and CPU. For example, when  $n = 256$ , Figure 7 shows the acceleration ratio of the GADI-AB method over the HSS scheme in terms of CPU time. To clearly demonstrate the acceleration ratio, we take the CPU

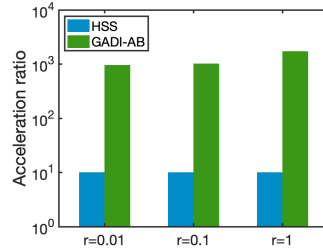


Fig. 7: The acceleration ratio of the GADI-AB against the HSS when  $n = 256$ .

cost of the HSS as a reference (set as “10”). As shown in Figure 7, the GADI-AB method spends much less CPU time than the HSS scheme does for different  $r$  with acceleration ratio 95.49 ( $r = 0.01$ ), 97.71 ( $r = 0.1$ ), and 170.92 ( $r = 1$ ). Figure 8 gives the corresponding convergent curves of HSS and GADI-AB.

These numerical results demonstrate that the HSS and the GADI-AB methods can efficiently solve the continuous Sylvester equation (2.22) with relatively optimal splitting parameters. And our proposed GADI-AB method indeed saves much more time compared with the HSS method. However, obtaining relatively optimal splitting parameters through the traversal method is expensive. For instance, when  $n = 128, r = 0.01$ , the HSS method takes over 6000 seconds to traverse  $\alpha$ . The traversal time will greatly increase as  $n$  increases. In the following, we will apply the GPR method to accelerate the GADI-AB method and calculate larger-scale matrix equations.

Analogously, we find that  $\omega$  is an insensitive parameter. Therefore we obtain a

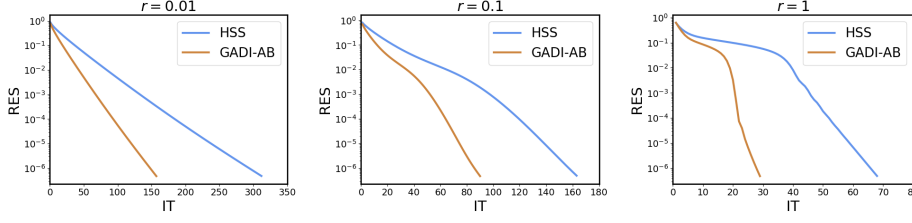


Fig. 8: The convergent curves of HSS and GADI-AB for solving the continuous Sylvester equation (2.22) when  $n = 256$ .

relatively optimal  $\omega_p$  through the traversing method for small-scale problems. And we use the GPR method to predict the relatively optimal  $\alpha$ . Table 10 gives the test, training, and retrained data sets. Figure 9 shows the parameter regression process of the GADI-AB method, and Table 11 presents the prediction results obtained through curves.  $\alpha_p$  denotes the prediction parameter obtained by the GPR method.

Table 10: The training, test, and retrained sets used in the GPR algorithm for the GADI-AB method.

	$r = 0.01$	$r = 0.1$	$r = 1$
Training set	$n : 4 \sim 20, \Delta n = 4$ $n : 24 \sim 72, \Delta n = 8$ $n : 80 \sim 112, \Delta n = 16$	$n : 4 \sim 20, \Delta n = 4$ $n : 24 \sim 72, \Delta n = 8$ $n : 80 \sim 112, \Delta n = 16$	$n : 4 \sim 20, \Delta n = 4$ $n : 24 \sim 72, \Delta n = 8$ $n : 80 \sim 112, \Delta n = 16$
Test set	$n : 1 \sim 500, \Delta n = 1$	$n : 1 \sim 500, \Delta n = 1$	$n : 1 \sim 1000, \Delta n = 1$
Retrained set	$n : 120 \sim 500,$ $\Delta n = 30$	$n : 120 \sim 500,$ $\Delta n = 10$	$n : 120 \sim 1000,$ $\Delta n = 50$

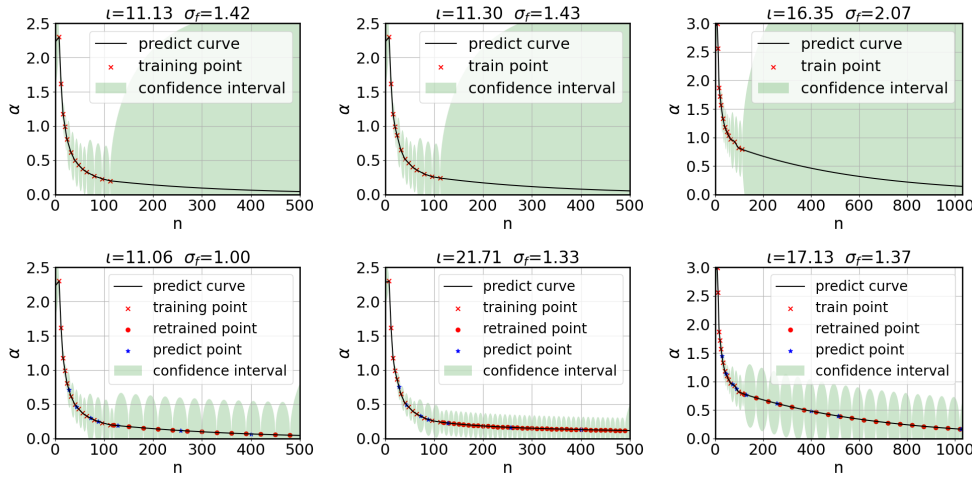


Fig. 9: The regression curve of  $\alpha$  for the GADI-AB method (Left:  $r = 0.01$ ; Middle:  $r = 0.1$ ; Right:  $r = 1$ ).



Table 11: Results of the GADI-AB method solving the continuous Sylvester equation by predicting parameter  $\alpha_p$  of GPR.

	$n$	$(\alpha_p, \omega_p)$	$IT_{\alpha_p}$	CPU(s)
$r = 0.01$	256	(0.1161,0.0)	200	0.4827
	400	(0.0651,0.0)	258	1.4994
	512	(0.0421,0.0)	319	4.6850
$r = 0.1$	256	(0.1621,0.0)	93	0.2348
	400	(0.1299,0.0)	110	0.5985
	512	(0.1144,0.0)	120	1.5475
	1024	(0.0668,0.0)	201	18.8272
$r = 1$	256	(0.6170,0.1)	30	0.0605
	400	(0.4808,0.1)	36	0.1706
	512	(0.3961,0.1)	40	0.3263
	1024	(0.1654,0.1)	92	6.6008
	2048	(0.0285,0.1)	534	289.6384

From Figure 9, we also find that putting the predicted data into a retrained set can shrink the confidence interval. Figure 9 and Table 11 show that the scale of the predictable  $n$  can reach 4.57 times ( $r = 0.01$ ), 9.14 times ( $r = 0.1$ ), and 18.29 times ( $r = 1$ ). These results demonstrate that the GPR method has a good generalization capability for solving the continuous Sylvester equation. The GPR method also provides an accurate optimal parameter prediction without an expensive consumption. The resulting method allows us to solve much larger Sylvester matrix equations (see Table 11) than these methods in Table 9 do through the traversal way to obtain relatively optimal splitting parameters.

To further demonstrate the performance of our proposed method, we also compare the existing ADI algorithms with the GADI-AB method for solving the continuous Sylvester equation (2.22). Table 12 summarizes these results. The data of other methods all come from corresponding references. From Table 12, one can find that the proposed GADI-AB method is the most efficient, tens to thousands of times faster than the existing methods even ignoring the consumption of obtaining a relatively optimal splitting parameters under almost the same hardware and software environments.

**5. Conclusions.** In this paper, we propose a GADI framework to solve large-scale sparse linear systems. The new proposed framework can unify most existing ADI methods, and can derive new methods as shown in Table 1. In this work, we present three new ADI methods, including the GADI-HS, the practical GADI-HS, and the GADI-AB schemes. To address the challenge of how to choose optimal splitting parameters of splitting methods, we present a data-driven method, the GPR method, to predict relatively optimal splitting parameters, which greatly improves the efficiency of ADI methods. Combining with the GADI framework and the GPR method, we can address large linear sparse systems within an efficient one-shot computation. Numerical results demonstrate that the proposed methods are faster by tens to thousands of times than the (inexact) HSS-type methods. Moreover, our proposed methods can solve much larger linear systems that these existing ADI methods have not reached.

There are still lots of works based on the proposed methods. For instance, one is to apply the GPR method to predicting optimal parameters for more splitting schemes. The second interesting work is to extend the GPR method to predict optimal multiparameter methods. The third one is to develop more efficient ADI schemes

Table 12: Results of ADI methods of solving continuous Sylvester equation with  $n = 256$ .

	Paper	Hardware Environment	Method	IT	CPU(s)
$r = 0.01$	[3]	—	HSS	203	44.67
	[3]	—	SOR	310	244.41
	[24]	1.4 GHz, 2GB RAM	HSS	518	1736.07
	[24]	1.4 GHz, 2GB RAM	TSS	288	1005.85
	[26]	2.2 GHz, 8GB RAM	NSS	118	20.12
	[15]	2.4 GHz, 2GB RAM	NSCG	287	101.05
	[15]	2.4 GHz, 2GB RAM	PNSCG	16	5.81
	<b>Our</b>	<b>2.3 GHz, 8GB RAM</b>	<b>GADI-AB</b>	<b>157</b>	<b>0.45</b>
$r = 0.1$	[3]	—	HSS	156	33.89
	[3]	—	SOR	304	236.69
	[24]	1.4 GHz, 2GB RAM	HSS	274	961.41
	[24]	1.4 GHz, 2GB RAM	TSS	227	813.45
	[15]	2.4 GHz, 2GB RAM	NSCG	170	61.22
	[15]	2.4 GHz, 2GB RAM	PNSCG	75	14.84
		<b>Our</b>	<b>2.3 GHz, 8GB RAM</b>	<b>GADI-AB</b>	<b>90</b>
$r = 1$	[3]	—	HSS	85	20.49
	[3]	—	SOR	256	205.23
	[24]	1.4 GHz, 2GB RAM	HSS	95	654.86
	[24]	1.4 GHz, 2GB RAM	TSS	84	269.89
	[26]	2.2 GHz, 8GB RAM	NSS	69	15.12
		<b>Our</b>	<b>2.3 GHz, 8GB RAM</b>	<b>GADI-AB</b>	<b>29</b>

from the proposed framework to solve much larger structured linear systems. The fourth interesting point is to extend the proposed methods to nonlinear systems.

**Acknowledgement.** We sincerely thank the editor and anonymous referees for the insightful comments and suggestions. Those comments are all valuable and very helpful for revising and improving our paper. We appreciate Qi Zhou for the kind help in revising our paper.

## Appendix A. Proofs..

### Appendix A.1. Proof of Lemma 2.7.

*Proof.* Set

$$(5.1) \quad \begin{cases} M_1 = \alpha I + H, & \begin{cases} M_2 = (S - \alpha I)[S - (1 - \omega)\alpha I]^{-1}(\alpha I + S), \\ N_2 = (S - \alpha I)[S - (1 - \omega)\alpha I]^{-1}(\alpha I + S) - A. \end{cases} \\ N_1 = \alpha I - S, \end{cases}$$

By using the first splitting scheme in (5.1), we have  $(\alpha I + H)\tilde{x}^{(k+\frac{1}{2})} = (\alpha I - S)\tilde{x}^{(k)} + b$ , i.e.,

$$(5.2) \quad \tilde{x}^{(k)} = (\alpha I - S)^{-1}[(\alpha I + H)\tilde{x}^{(k+\frac{1}{2})} - b].$$

Additionally, from the practical GADI framework (2.12), we have

$$(5.3) \quad [S - (1 - \omega)\alpha I]^{-1}(\alpha I + S)\tilde{x}^{(k+1)} = \tilde{x}^{(k)} + [S - (1 - \omega)\alpha I]^{-1}(2 - \omega)\alpha\tilde{x}^{(k+\frac{1}{2})}.$$

We substitute (5.2) into (5.3), and utilize the practical GADI framework (2.12) to obtain  $\tilde{x}^{(k+1)}$

$$\begin{aligned} & (S - \alpha I)[S - (1 - \omega)\alpha I]^{-1}(\alpha I + S)\tilde{x}^{(k+1)} \\ &= (S - \alpha I)[S - (1 - \omega)\alpha I]^{-1}(\alpha I + S)\tilde{x}^{(k+\frac{1}{2})} - A\tilde{x}^{(k+\frac{1}{2})} + b. \end{aligned}$$

Considering the second splitting in (5.1), it is evident that

$$M_2 \tilde{x}^{(k+1)} = N_2 \tilde{x}^{(k+\frac{1}{2})} + b.$$

This implies that the practical GADI framework (Algorithm 2.1) is equivalent to the assumption conditions (2.14). Using (2.14), we have

$$\begin{aligned} \tilde{x}^{(k+1)} &= \tilde{x}^{(k+\frac{1}{2})} + M_2^{-1}(\tilde{r}^{(k+\frac{1}{2})} + \tilde{q}^{(k+\frac{1}{2})}) = M_2^{-1}N_2\tilde{x}^{(k+\frac{1}{2})} + M_2^{-1}b + M_2^{-1}\tilde{q}^{(k+\frac{1}{2})} \\ &= M_2^{-1}N_2[\tilde{x}^{(k)} + M_1^{-1}(\tilde{r}^{(k)} + \tilde{p}^{(k)})] + M_2^{-1}b + M_2^{-1}\tilde{q}^{(k+\frac{1}{2})} \\ &= M_2^{-1}N_2M_1^{-1}N_1\tilde{x}^{(k)} + M_2^{-1}(N_2M_1^{-1} + I)b + M_2^{-1}(N_2M_1^{-1}\tilde{p}^{(k)} + \tilde{q}^{(k+\frac{1}{2})}), \end{aligned}$$

i.e., (2.15). Thus, we complete the proof.  $\square$

### Appendix A.2. Proof of Lemma 3.3.

*Proof.* By (2.8) and the similarity invariance of matrix spectrum, we obtain

$$\begin{aligned} \rho(T(\alpha, \omega)) &= \rho((\alpha I + S)^{-1}(\alpha I + H)^{-1}(\alpha^2 I + HS - (1 - \omega)\alpha A)) \\ &\leq \alpha \|(\alpha I + S)^{-1}(\alpha I + H)^{-1}(\alpha I - (1 - \omega)A)\|_2 + \|(\alpha I + S)^{-1}(\alpha I + H)^{-1}HS\|_2 \\ &\leq \alpha \|(\alpha I + S)^{-1}\|_2 \|(\alpha I + H)^{-1}\|_2 (\alpha + |1 - \omega| \|A\|_2) + \|(\alpha I + H)^{-1}H\|_2 \|S(\alpha I + S)^{-1}\|_2. \blacksquare \end{aligned}$$

Scaling the last two items appropriately yields

$$\begin{aligned} &\alpha \|(\alpha I + S)^{-1}\|_2 \|(\alpha I + H)^{-1}\|_2 (\alpha + |1 - \omega| \|A\|_2) \\ &= \alpha \max_{\lambda_i \in \lambda(H)} \left| \frac{1}{\alpha + \lambda_i} \right| \max_{\sigma_i \in \sigma(S)} \left| \frac{1}{\sqrt{\alpha^2 + \sigma_i^2}} \right| (\alpha + |1 - \omega| \|A\|_2) \\ &\leq \frac{\alpha}{\alpha + \lambda_{min}} \cdot \frac{1}{\alpha} (\alpha + |1 - \omega| \|A\|_2) = \frac{\alpha + |1 - \omega| \|A\|_2}{\alpha + \lambda_{min}}. \end{aligned}$$

Since  $H$  is a Hermitian positive definite matrix, then  $\lambda_i > 0$  and

$$\begin{aligned} &\|(\alpha I + H)^{-1}H\|_2 \|S(\alpha I + S)^{-1}\|_2 \\ &= \max_{\lambda_i \in \lambda(H)} \left| \frac{\lambda_i}{\alpha + \lambda_i} \right| \max_{\sigma_i \in \sigma(S)} \left| \frac{\sigma_i}{\sqrt{\alpha^2 + \sigma_i^2}} \right| = \frac{\lambda_{max}}{\alpha + \lambda_{max}} \cdot \frac{\sigma_{max}}{\sqrt{\alpha^2 + \sigma_{max}^2}} \leq \frac{\lambda_{max}\sigma_{max}}{(\alpha + \lambda_{min})\alpha}. \end{aligned}$$

Therefore, we obtain  $\square$

$$\rho(T(\alpha, \omega)) \leq \frac{\alpha^2 + \alpha|1 - \omega| \|A\|_2 + \lambda_{max}\sigma_{max}}{\alpha(\alpha + \lambda_{min})}.$$

### Appendix A.3. Proof of Theorem 3.5.

*Proof.* (i) From Theorem 2.5(i), when  $|\lambda_k|^2 \leq a$  and  $0 \leq \omega < 2$ , then

$$\rho(M(\alpha)) \leq \rho(T(\alpha, \omega)) < 1.$$

If  $\alpha^*$  and  $\omega^*$  are the quasi-optimal parameters in this case, we have

$$\rho(T(\alpha^*, \omega^*)) = \rho(M(\alpha^*)).$$

Furthermore, due to  $\rho(T(\alpha, 0)) = \rho(M(\alpha))$  and (2.5), it is obvious that

$$\omega^* = \operatorname{argmin}_{\omega} \left\{ \frac{1}{2} [\omega + (2 - \omega)\sigma(\alpha)] \right\} = 0.$$

The GADI-HS method reduces to the HSS iterative method, from [Lemma 3.4](#); then

$$\alpha^* = \operatorname{argmin}_{\alpha} \left\{ \frac{1}{2} [\omega + (2 - \omega)\sigma(\alpha)] \right\} = \operatorname{argmin}_{\alpha} \left\{ \sigma(\alpha) \right\} = \sqrt{\lambda_{\min} \lambda_{\max}}.$$

(ii) From [Theorem 2.5\(ii\)](#), when  $a < |\lambda_k|^2$  and  $0 < \omega < \frac{4a^2 - 4a + 4b^2}{(1-a)^2 + b^2}$ , we have

$$\rho(T(\alpha, \omega)) < \rho(M(\alpha)) < 1.$$

Thus, we consider the bound of  $\rho(T(\alpha, \omega))$  in inequality [\(3.5\)](#)

$$\rho(T(\alpha, \omega)) \leq \delta(\alpha, \omega) = \frac{\alpha^2 + \alpha|1 - \omega|\|A\|_2 + \lambda_{\max}\sigma_{\max}}{\alpha(\alpha + \lambda_{\min})}.$$

Our objective is to minimize  $\delta(\alpha, \omega)$ .

When  $\alpha$  is fixed,  $\delta(\alpha, \omega)$  reaches the minimum at  $w = 1$

$$\omega^* = \operatorname{argmin}_{\omega} \{\delta(\alpha, \omega)\} = 1,$$

then

$$(5.4) \quad \alpha^* = \operatorname{argmin}_{\alpha} \left\{ \frac{\alpha^2 + \lambda_{\max}\sigma_{\max}}{\alpha(\alpha + \lambda_{\min})} \right\} := \operatorname{argmin}_{\alpha} \left\{ \frac{\alpha^2 + p}{\alpha(\alpha + \lambda_{\min})} \right\},$$

where  $p = \lambda_{\max}\sigma_{\max}$ . The first-order optimal condition of [\(5.4\)](#) means

$$\frac{\partial \delta(\alpha, 1)}{\partial \alpha} = \frac{2\alpha(\alpha^2 + \alpha\lambda_{\min}) - (\alpha^2 + p)(2\alpha + \lambda_{\min})}{(\alpha + \lambda_{\min})^2 \alpha^2} = 0.$$

Solving the above equation,  $\alpha^* = \operatorname{argmin}_{\alpha} \{\delta(\alpha, \omega)\} = \frac{p + \sqrt{p^2 + \lambda_{\min}^2 p}}{\lambda_{\min}}$ . From [\(5.4\)](#), we have

$$\delta(\alpha^*, \omega^*) = \frac{2p^2 + 2\lambda_{\min}^2 p + 2p\sqrt{p^2 + \lambda_{\min}^2 p}}{2p^2 + 2\lambda_{\min}^2 p + 2p\sqrt{p^2 + \lambda_{\min}^2 p} + \lambda_{\min}^2 \sqrt{p^2 + \lambda_{\min}^2 p}} < 1. \quad \square$$

**Appendix A.4: Two-dimensional parabolic equation.** Two-dimensional parabolic equation Consider the following 2D parabolic equation

$$(5.5) \quad -u_{x_1 x_1} - u_{x_2 x_2} + 2u_{x_1 x_2} + u_{x_1} = f(x_1, x_2), \quad (x_1, x_2) \in \Omega,$$

on the unit cube  $\Omega = [0, 1] \times [0, 1]$  with homogeneous Dirichlet boundary condition. We use the centered difference method to discretize the parabolic equation [\(5.5\)](#), and obtain the linear system  $Ax = b$ . The coefficient matrix is

$$(5.6) \quad A = I \otimes T_1 + D_1 \otimes T_2 + D_2 \otimes T_3,$$

where  $D_1, D_2, T_1, T_2, T_3$  are tridiagonal matrices defined by

$$D_1 = \operatorname{Tridiag}(0, 0, 1), \quad D_2 = \operatorname{Tridiag}(1, 0, 0), \quad T_1 = \operatorname{Tridiag}(-1 - \beta, 4, -1 + \beta),$$

$$T_2 = \operatorname{Tridiag}(-1/2, -1, 1/2), \quad T_3 = \operatorname{Tridiag}(1/2, -1, -1/2), \quad \beta = 1/(2n + 2),$$

Table 13: A comparison of the HSS and the GADI-HS methods for solving 2D parabolic equation with theoretical quasi-optimal splitting parameters.

$n^2$	HSS			GADI-HS		
	$\alpha_q$	IT	CPU(s)	$(\alpha_q, \omega_q)$	IT	CPU(s)
$16^2$	0.6156	77	0.0054	(0.1158, 1.0)	37	0.0035
$32^2$	0.3050	140	0.1243	(0.0603, 1.0)	64	0.0580
$64^2$	0.1501	257	4.8332	(0.0307, 1.0)	114	2.1430
$96^2$	0.0991	373	35.6514	(0.0206, 1.0)	163	15.8759

with  $n$  is the degree of freedom along each dimension.  $x \in \mathbb{R}^{n^2}$  is the unknown vector of discretizing  $u(x_1, x_2)$ .  $b \in \mathbb{R}^{n^2}$  is the discretization vector of  $f(x_1, x_2)$  which is determined by choosing the exact solution  $u(x_1, x_2) = \sin(\pi x_1) \sin(\pi x_2)$ . All tests are started with the zero vector. All iterative methods are terminated if the relative residual error satisfies  $\text{RES} = \|r^{(k)}\|_2 / \|r^{(0)}\|_2 \leq 10^{-6}$ , where  $r^{(k)} = b - Ax^{(k)}$  is the  $k$ -step residual.

Firstly, we compare the performance of the GADI-HS and the HSS in solving the above linear algebra equation  $Ax = b$ . The parameters in the HSS and the GADI-HS methods are obtained from Lemma 3.4 and Theorem 3.5, respectively. Table 13 presents corresponding numerical results, where ‘‘IT’’ and ‘‘CPU’’ denote the required iterations and the CPU time (in seconds), respectively. From Table 13, one can find that the GADI-HS method spends less than half of CPU times compared with the HSS method. It is consistent with the prediction by Theorem 3.5 that shows the convergence speed of the GADI-HS scheme is faster than the HSS method. These results demonstrate that the GADI-HS scheme derived from the new GADI framework accelerates the convergence speed in solving (5.5).

Next, we use the Practical GADI-HS and the IHSS methods to solve much larger linear systems. Meanwhile, we employ the GPR method to predict the splitting parameters in the Practical GADI-HS method. The inner iteration is terminated if residuals satisfy

$$\|p^{(k)}\|_2 \leq 1 \times 10^{-\delta_H} \|r^{(k)}\|_2, \quad \|q^{(k)}\|_2 \leq 1 \times 10^{-\delta_S} \|r^{(k+\frac{1}{2})}\|_2,$$

where  $\delta_H$  and  $\delta_S$  are controllable tolerances in the inner iteration to balance the Hermitian and skew-Hermitian parts in the linear sub-problems. In these tests, we set  $\delta_H = \delta_S = 2$ .

For the IHSS method, there has been no theoretical approach to estimate splitting parameters. Alternatively, the splitting parameters can be obtained by traversing method or by the GRP method. Section 4.1.3 has demonstrated that the GRP method can predict accurate splitting parameter of IHSS method as the traversing method does. Here, we still use the traversing method to obtain the relatively accurate splitting parameter  $\alpha^*$  in traversing interval  $(0, 3]$  with a step size of 0.01. And we use the GPR method to predict the splitting parameter  $\alpha$  for the Practical GADI-HS scheme. Table 14 gives the training, test, and retrained data sets.  $\alpha$  in the training data set of the GPR approach is produced by traversing parameters, but only for small-scale linear systems,  $n$  from 2 to 100 with different step size  $\Delta n$ , as shown in Table 14. Figure 10 shows the optimal parameter regression and prediction processes for the Practical GADI-HS method. From the Figure 10, we can find that adding retrained data set in training can improve the prediction accuracy and strengthen the generalization ability of the regression model. Meanwhile, we find that the parameter  $\omega$

in the Practical GADI-HS method is insensitive to the scale of the matrix. Therefore, we obtain the optimal  $\omega_p$  by the traversing method for small-scale problems.

Table 14: The training, test and retrained sets of the Practical GADI-HS method in GPR algorithm.

Training set	$n : 6 \sim 10, \Delta n = 2$ $n : 12 \sim 24, \Delta n = 4$ $n : 32 \sim 72, \Delta n = 8$ $n : 80 \sim 100, \Delta n = 10$
Test set	$n : 1 \sim 200, \Delta n = 1$
Retrained set	$n : 110 \sim 200, \Delta n = 10$

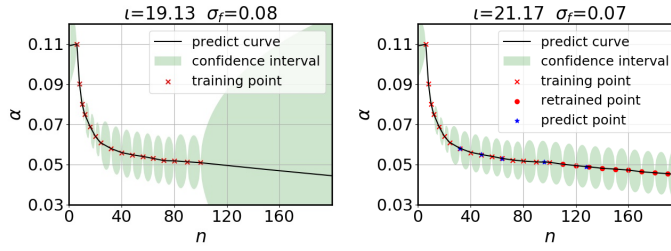


Fig. 10: The regression curve of  $\alpha$  against  $n$  for the Practical GADI-HS method.

Table 15 shows the numerical results obtained by the IHSS and the Practical GADI-HS methods for different scale discretization systems.  $IT_{CG}$  and  $IT_{CGNE}$  denote the iterations for solving sub-systems in inexact methods. These results demonstrate that the IHSS method can solve relatively large linear systems with less CPU times than the HSS algorithm does when the relatively optimal parameter  $\alpha^*$  is used. However, obtaining  $\alpha^*$  in the IHSS costs lots of traversal times, as shown in the last column in Table 15. For example, when  $n = 64^3$ , the traversal time of the IHSS method is about 15000 seconds. Compared with the IHSS method, the Practical

Table 15: Results of the IHSS method ( $\alpha^*$  obtained by traversing interval  $(0, 3]$  with a step size of 0.01) and the Practical GADI-HS method (relatively optimal parameters  $(\alpha_p, \omega_p)$  obtained by the GPR algorithm) for solving 2D parabolic equation.

Method	$n^2$	$\alpha^*$	IT ( $IT_{CG}, IT_{CGNE}$ )	CPU (s)	traversal CPU(s)
IHSS	$32^2(1024)$	0.92	403 (3.00, 1.00)	0.08	2835.17
	$48^2(2304)$	0.91	853 (3.00, 1.00)	0.36	6011.50
	$64^2(4096)$	0.91	1460 (3.00, 1.00)	1.76	14881.66
	$n^2$	$(\alpha_p, \omega_p)$	IT ( $IT_{CG}, IT_{CGNE}$ )	CPU (s)	traversal CPU(s)
Practical GADI-HS	$32^2(1024)$	(0.0578, 1.9)	34 (20.00, 2.00)	0.05	0
	$48^2(2304)$	(0.0549, 1.9)	60 (23.00, 1.00)	0.12	0
	$64^2(4096)$	(0.0528, 1.9)	98 (23.00, 1.00)	0.35	0
	$96^2(9216)$	(0.0512, 1.9)	203 (20.00, 1.00)	1.71	0
	$128^2(16384)$	(0.0492, 1.9)	350 (18.00, 1.00)	4.02	0
	$256^2(65536)$	(0.0430, 1.9)	1325 (12.00, 1.00)	70.53	0

GADI-HS scheme is much more efficient in combination with the GPR approach. As an example, Figure 11 gives the convergent curve when  $n^2 = 64^2$ . Therefore in the practical (online) computation, the Practical GADI-HS scheme can obtain the solution with an efficient one-shot computation and does not consume traversal CPU time anymore. And with accurately predicted  $\alpha$ , the Practical GADI-HS method can efficiently solve large linear systems.

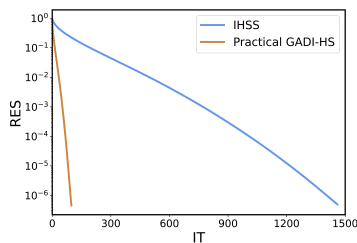


Fig. 11: The convergent curves of the IHSS and the Practical GADI-HS in solving 2D parabolic equation when  $n^2 = 64^2$ .

**Acknowledgments.** We sincerely thank the editor and anonymous referees for the insightful comments and suggestions. Those comments are all valuable and very helpful for revising and improving our paper. We appreciate Qi Zhou for the kind help in revising our paper.

#### REFERENCES

- [1] N. AGHAZADEH, D. K. SALKUYEH, AND M. BASTANI, *Two-parameter generalized hermitian and skew-hermitian splitting iteration method*, International journal of computer mathematics, 93 (2016), pp. 1119–119.
- [2] O. AXELSSON, Z. BAI, AND S. QIU, *A class of nested iteration schemes for linear systems with a coefficient matrix with a dominant positive definite symmetric part*, Numerical Algorithms, 35 (2004), pp. 351–372.
- [3] Z.-Z. BAI, *On hermitian and skew-hermitian splitting iteration methods for continuous sylvester equations*, Journal of Computational Mathematics, (2011), pp. 185–198.
- [4] Z.-Z. BAI, G. H. GOLUB, AND M. K. NG, *Hermitian and skew-hermitian splitting methods for non-hermitian positive definite linear systems*, SIAM Journal on Matrix Analysis and Applications, 24 (2003), pp. 603–626.
- [5] Z. Z. BAI, G. H. GOLUB, AND M. K. NG, *On successive-overrelaxation acceleration of the hermitian and skew-hermitian splitting iterations*, Numerical Linear Algebra with Applications, 14 (2007), pp. 319–335.
- [6] Z.-Z. BAI AND J.-Y. PAN, *Matrix Analysis and Computations*, SIAM, 2021.
- [7] P. BENNER, R. LI, AND N. TRUHAR, *On the adi method for sylvester equations*, Journal of Computational and Applied Mathematics, 233 (2009), pp. 1035–1045.
- [8] M. BENZI, M. GANDER, AND G. H. GOLUB, *Optimization of the hermitian and skew-hermitian splitting iteration for saddle-point problems*, BIT Numerical Mathematics, 43 (2003), pp. 881–900.
- [9] D. BERTACCINI, G. H. GOLUB, S. S. CAPIZZANO, AND C. T. POSSIO, *Preconditioned hss methods for the solution of non-hermitian positive definite linear systems and applications to the discrete convection-diffusion equation*, Numerische Mathematik, 99 (2005), pp. 441–484.
- [10] Y. CAO, Z. REN, AND L. YAO, *Improved relaxed positive-definite and skew-hermitian splitting preconditioners for saddle point problems*, Journal of Computational Mathematics, 37 (2019).
- [11] J. DOUGLAS AND H. H. RACHFORD, *On the numerical solution of heat conduction problems in two and three space variables*, Transactions of the American mathematical Society, 82

- (1956), pp. 421–439.
- [12] J. ECKSTEIN AND D. P. BERTSEKAS, *On the douglas—rachford splitting method and the proximal point algorithm for maximal monotone operators*, *Mathematical Programming*, 55 (1992), pp. 293–318.
  - [13] J. FRIEDMAN, T. HASTIE, AND R. TIBSHIRANI, *The Elements of Statistical Learning*, Springer, 2000.
  - [14] C. GREIF AND J. VARAH, *Iterative solution of cyclically reduced systems arising from discretization of the three-dimensional convection-diffusion equation*, *SIAM Journal on Scientific Computing*, 19 (1998), pp. 1918–1940.
  - [15] Y. KE AND C. MA, *A preconditioned nested splitting conjugate gradient iterative method for the large sparse generalized sylvester equation*, *Computers & Mathematics with Applications*, 68 (2014), pp. 1409–1420.
  - [16] P.-L. LIONS AND B. MERCIER, *Splitting algorithms for the sum of two nonlinear operators*, *SIAM Journal on Numerical Analysis*, 16 (1979), pp. 964–979.
  - [17] G. I. MARCHUK, *Splitting and alternating direction methods*, *Handbook of Numerical Analysis*, 1 (1990), pp. 197–462.
  - [18] D. W. PEACEMAN AND H. H. RACHFORD, JR, *The numerical solution of parabolic and elliptic differential equations*, *Journal of the Society for industrial and Applied Mathematics*, 3 (1955), pp. 28–41.
  - [19] T. PENZL, *A cyclic low-rank smith method for large sparse lyapunov equations*, *SIAM Journal on Scientific Computing*, 21 (1999), pp. 1401–1418.
  - [20] C. E. RASMUSSEN AND H. NICKISCH, *Gaussian processes for machine learning (gpml) toolbox*, *Journal of Machine Learning Research*, 11 (2010), pp. 3011–3015.
  - [21] G. STRANG, *A proposal for toeplitz matrix calculations*, *Studies in Applied Mathematics*, 74 (1986), pp. 171–176.
  - [22] A. THEMELIS AND P. PATRINOS, *Douglas—rachford splitting and admm for nonconvex optimization: Tight convergence results*, *SIAM Journal on Optimization*, 30 (2020), pp. 149–181.
  - [23] R. S. VARGA, *Matrix iterative analysis, Second Edition*, Springer, 1999.
  - [24] X. WANG, W.-W. LI, AND L.-Z. MAO, *On positive-definite and skew-hermitian splitting iteration methods for continuous sylvester equation  $ax+xb=c$* , *Computers & Mathematics with Applications*, 66 (2013), pp. 2352–2361.
  - [25] Z.-Q. WANG, J.-F. YIN, AND Q.-Y. DOU, *Preconditioned modified hermitian and skew-hermitian splitting iteration methods for fractional nonlinear schrödinger equations*, *Journal of Computational and Applied Mathematics*, 367 (2020), p. 112420.
  - [26] Q.-Q. ZHENG AND C.-F. MA, *On normal and skew-hermitian splitting iteration methods for large sparse continuous sylvester equations*, *Journal of Computational and Applied Mathematics*, 268 (2014), pp. 145–154.